



EFFECT OF BINARIES ON DARK MATTER ESTIMATES IN DWARF GALAXIES

Caveats to Dwarf Galaxy Indirect Detection Limits

LAURA J. CHANG

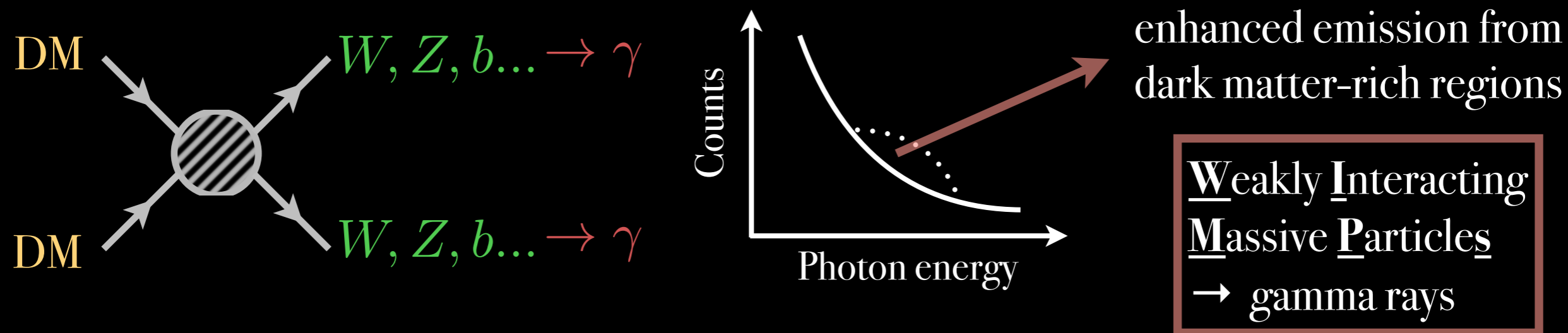
PRINCETON UNIVERSITY

Small Galaxies, Cosmic Questions

July 31, 2019

IN COLLABORATION WITH: LINA NECIB (CALTECH)

THERMAL WIMP DARK MATTER (DM)



Indirect detection

Fermi Large Area Telescope (*Fermi*-LAT)

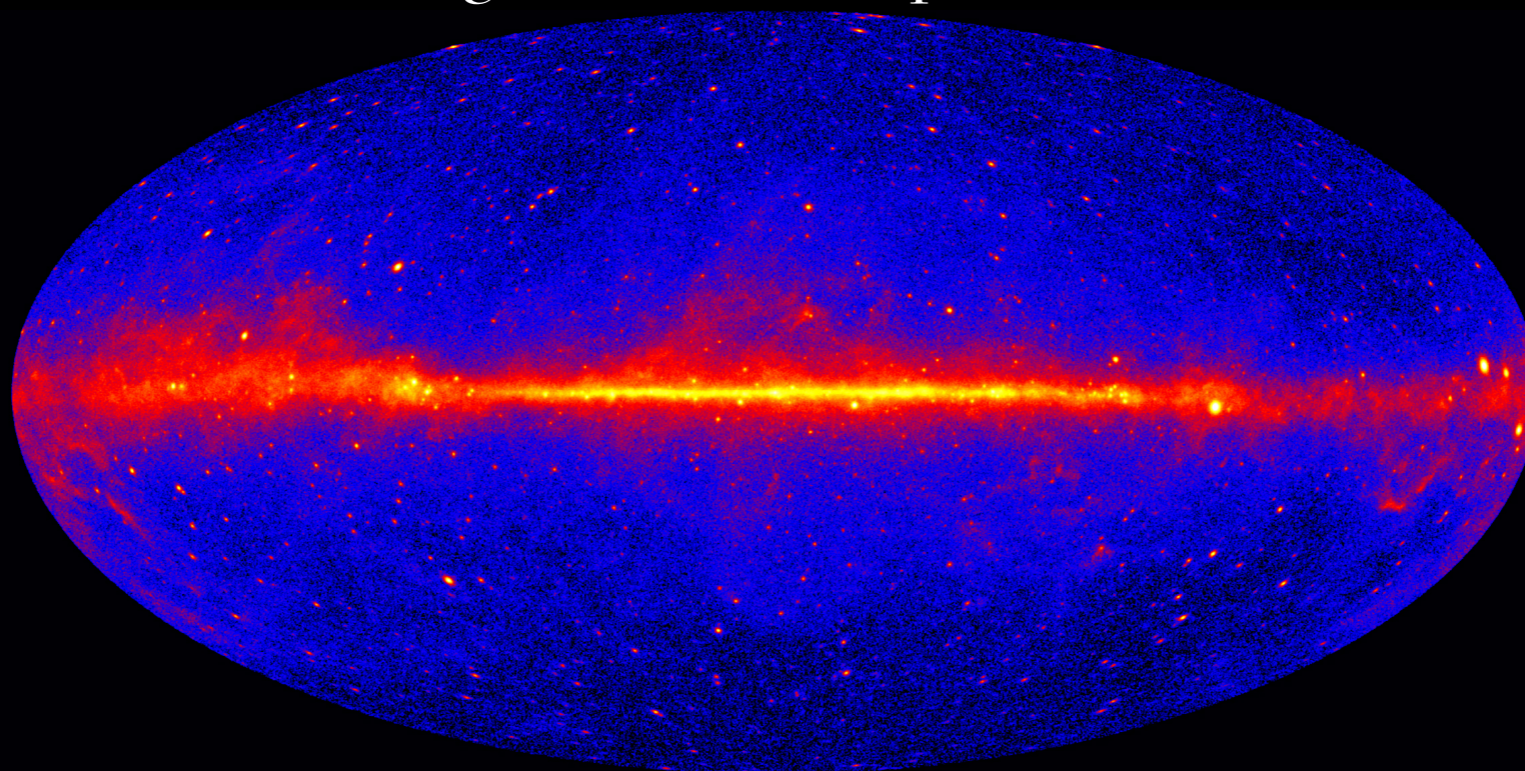
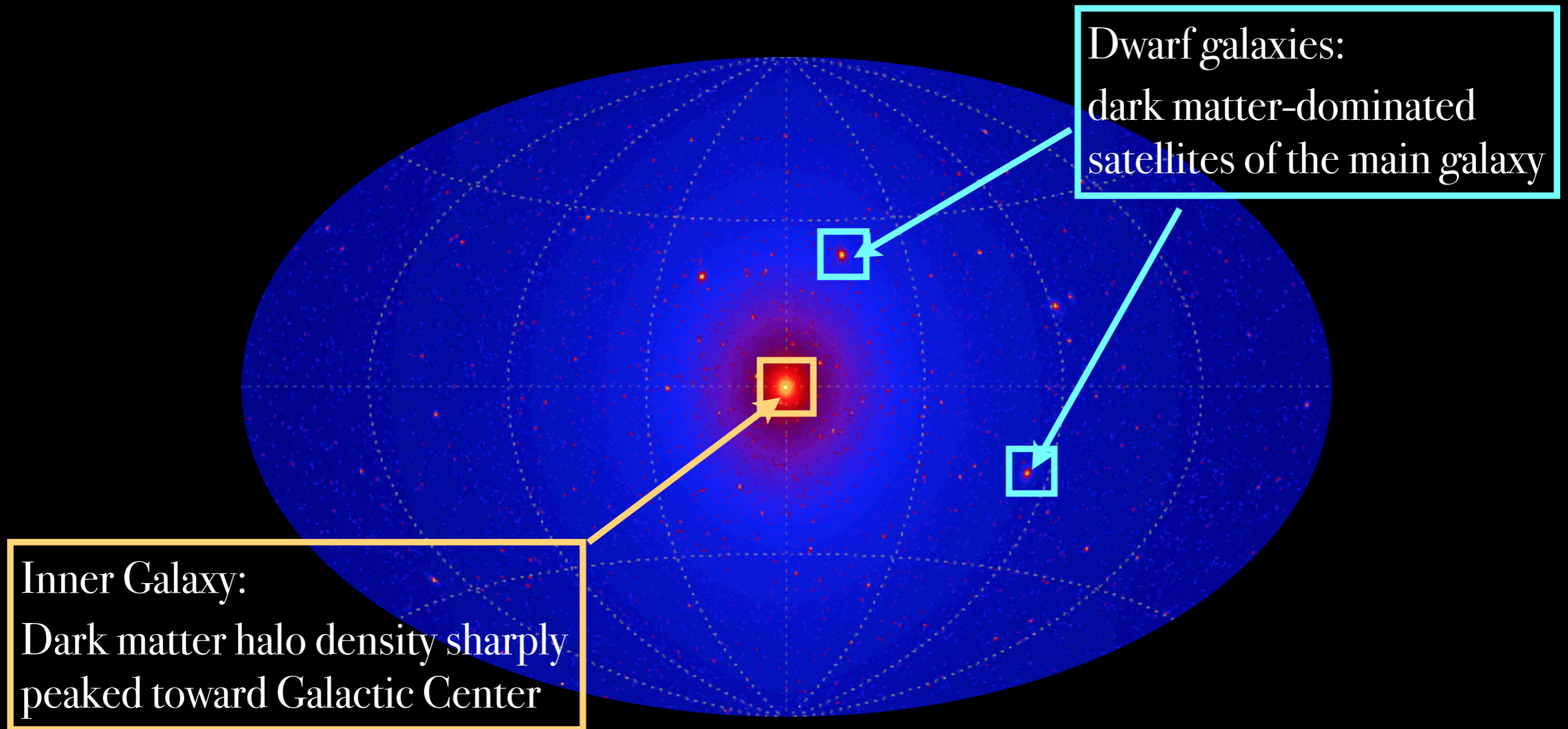


Image: NASA, DOE, *Fermi*-LAT collaboration

DARK MATTER ANNIHILATION IN THE SKY

$$\Phi_\gamma(\Delta\Omega) = \underbrace{\frac{1}{4\pi} \frac{\langle\sigma v\rangle}{2m_{\text{DM}}^2} \int_{E_{\text{min}}}^{E_{\text{max}}} \frac{dN_\gamma}{dE_\gamma} dE_\gamma}_{\text{particle physics}} \times \underbrace{\int_{\Delta\Omega} \int_{\text{l.o.s.}} \rho_{\text{DM}}^2(\mathbf{r}) dl d\Omega'}_{\text{astrophysics (J-factor)}}$$



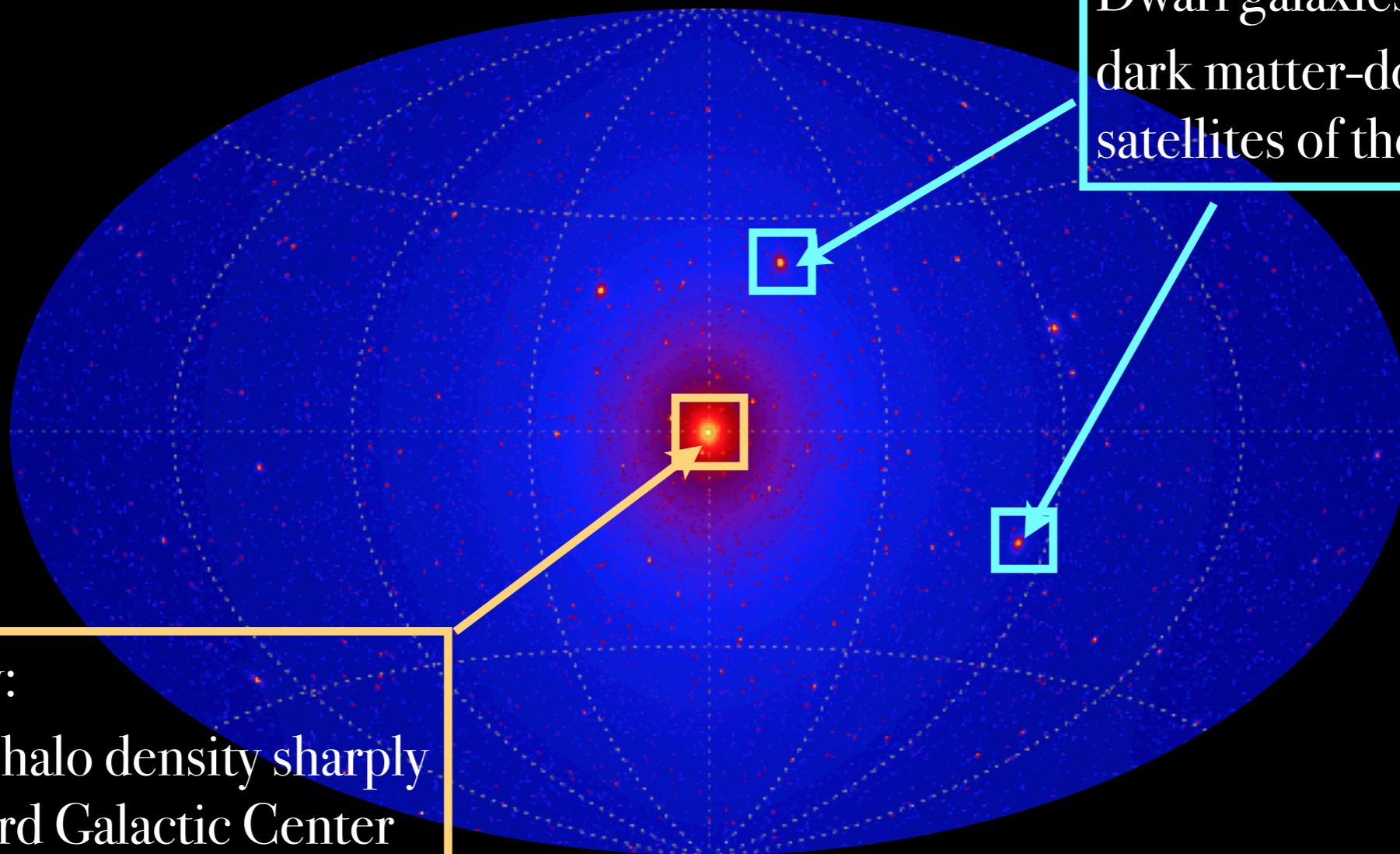
L. Pieri et al. [0908.0195]

DARK MATTER ANNIHILATION IN THE SKY

$$\Phi_\gamma(\Delta\Omega) = \underbrace{\frac{1}{4\pi} \frac{\langle\sigma v\rangle}{2m_{\text{DM}}^2} \int_{E_{\text{min}}}^{E_{\text{max}}} \frac{dN_\gamma}{dE_\gamma} dE_\gamma}_{\text{particle physics}} \times \underbrace{\int_{\Delta\Omega} \int_{\text{l.o.s.}} \rho_{\text{DM}}^2(\mathbf{r}) dl d\Omega'}_{\text{astrophysics (J-factor)}}$$

Inner Galaxy:
Dark matter halo density sharply peaked toward Galactic Center

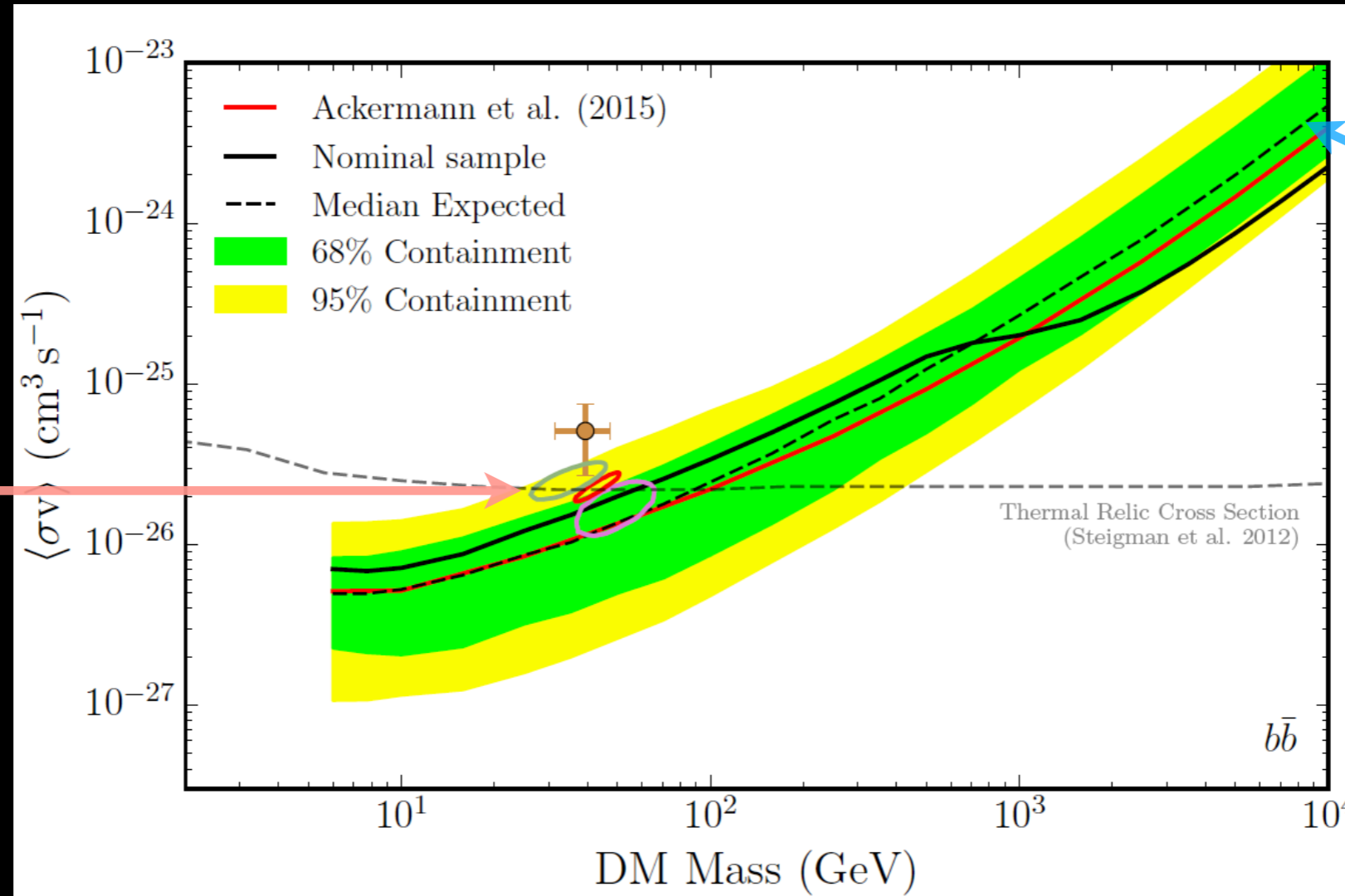
Dwarf galaxies:
dark matter-dominated satellites of the main galaxy



L. Pieri et al. [0908.0195]

INDIRECT DETECTION BENCHMARK: DWARF GALAXIES

- Low astrophysical backgrounds (dust/gas) compared to other indirect detection targets
→ some of the most stringent and robust constraints



Galactic Center Excess (GCE), dark matter interpretation

Analyze blank regions of the sky (no systematics)

Fermi-LAT collaboration and DES collaboration [1611.03184]

DWARF GALAXY INDIRECT DETECTION CAVEATS

(1) Name	(2) l, b (deg, deg)	(3) Distance (kpc)	(4) $r_{1/2}$ (pc)	(5) M_V (mag)	(6) $\log_{10}(J_{\text{meas}})$ $\log_{10}(\text{GeV}^2 \text{cm}^{-5})$	(7) $\log_{10}(J_{\text{pred}})$ $\log_{10}(\text{GeV}^2 \text{cm}^{-5})$
Kinematically Confirmed Galaxies						
Boötes I*	358.08, 69.62	66	189	-6.3	18.2 ± 0.4	18.5
Boötes II	353.69, 68.87	42	46	-2.7	...	18.9
Boötes III	35.41, 75.35	47	...	-5.8	...	18.8
Canes Venatici I	74.31, 79.82	218	441	-8.6	17.4 ± 0.3	17.4
Canes Venatici II*	113.58, 82.70	160	52	-4.9	17.6 ± 0.4	17.7
Carina*	260.11, -22.22	105	205	-9.1	17.9 ± 0.1	18.1
Coma Berenices*	241.89, 83.61	44	60	-4.1	19.0 ± 0.4	18.8
Draco*	86.37, 34.72	76	184	-8.8	18.8 ± 0.1	18.3
Draco II	98.29, 42.88	24	16	-2.9	...	19.3
Fornax*	237.10, -65.65	147	594	-13.4	17.8 ± 0.1	17.8
Hercules*	28.73, 36.87	132	187	-6.6	16.9 ± 0.7	17.9
Horologium I	271.38, -54.74	87	61	-3.5	...	18.2
Hydra II	295.62, 30.46	134	66	-4.8	...	17.8
Leo I	225.99, 49.11	254	223	-12.0	17.8 ± 0.2	17.3
Leo II*	220.17, 67.23	233	164	-9.8	18.0 ± 0.2	17.4
Leo IV*	265.44, 56.51	154	147	-5.8	16.3 ± 1.4	17.7
Leo V	261.86, 58.54	178	95	-5.2	16.4 ± 0.9	17.6
Pisces II	79.21, -47.11	182	45	-5.0	...	17.6
Reticulum II	266.30, -49.74	32	35	-3.6	18.9 ± 0.6	19.1
Sculptor*	287.53, -83.16	86	233	-11.1	18.5 ± 0.1	18.2
Segue 1*	220.48, 50.43	23	21	-1.5	19.4 ± 0.3	19.4
Sextans*	243.50, 42.27	86	561	-9.3	17.5 ± 0.2	18.2
Triangulum II	140.90, -23.82	30	30	-1.8	...	19.1
Tucana II	328.04, -52.35	58	120	-3.9	...	18.6
Ursa Major I	159.43, 54.41	97	143	-5.5	17.9 ± 0.5	18.1
Ursa Major II*	152.46, 37.44	32	91	-4.2	19.4 ± 0.4	19.1
Ursa Minor*	104.97, 44.80	76	120	-8.8	18.9 ± 0.2	18.3
Willman 1*	158.58, 56.78	38	19	-2.7	...	18.9
Likely Galaxies						
Columba I	231.62, -28.88	182	101	-4.5	...	17.6
Eridanus II	249.78, -51.65	331	156	-7.4	...	17.1
Grus I	338.68, -58.25	120	60	-3.4	...	17.9
Grus II	351.14, -51.94	53	93	-3.9	...	18.7
Horologium II	262.48, -54.14	78	33	-2.6	...	18.3
Indus II	354.00, -37.40	214	181	-4.3	...	17.4
Pegasus III	69.85, -41.81	205	57	-4.1	...	17.5
Phoenix II	323.69, -59.74	96	33	-3.7	...	18.1
Pictor I	257.29, -40.64	126	44	-3.7	...	17.9
Reticulum III	273.88, -45.65	92	64	-3.3	...	18.2
Sagittarius II	18.94, -22.90	67	34	-5.2	...	18.4
Tucana III	315.38, -56.18	25	44	-2.4	...	19.3
Tucana IV	313.29, -55.29	48	128	-3.5	...	18.7
Ambiguous Systems						
Cetus II	156.47, -78.53	30	17	0.0	...	19.1
Eridanus III	274.95, -59.60	96	12	-2.4	...	18.1
Kim 2	347.16, -42.07	105	12	-1.5	...	18.1
Tucana V	316.31, -51.89	55	16	-1.6	...	18.6

Fermi-LAT collaboration and DES collaboration [1611.03184]

DWARF GALAXY INDIRECT DETECTION CAVEATS

- Constraints rely on accurate J-factors

(1) Name	(2) l, b (deg, deg)	(3) Distance (kpc)	(4) $r_{1/2}$ (pc)	(5) M_V (mag)	(6) $\log_{10}(J_{\text{meas}})$ $\log_{10}(\text{GeV}^2 \text{cm}^{-5})$	(7) $\log_{10}(J_{\text{pred}})$ $\log_{10}(\text{GeV}^2 \text{cm}^{-5})$
Kinematically Confirmed Galaxies						
Boötes I*	358.08, 69.62	66	189	-6.3	18.2 ± 0.4	18.5
Boötes II	353.69, 68.87	42	46	-2.7	...	18.9
Boötes III	35.41, 75.35	47	...	-5.8	...	18.8
Canes Venatici I	74.31, 79.82	218	441	-8.6	17.4 ± 0.3	17.4
Canes Venatici II*	113.58, 82.70	160	52	-4.9	17.6 ± 0.4	17.7
Carina*	260.11, -22.22	105	205	-9.1	17.9 ± 0.1	18.1
Coma Berenices*	241.89, 83.61	44	60	-4.1	19.0 ± 0.4	18.8
Draco*	86.37, 34.72	76	184	-8.8	18.8 ± 0.1	18.3
Draco II	98.29, 42.88	24	16	-2.9	...	19.3
Fornax*	237.10, -65.65	147	594	-13.4	17.8 ± 0.1	17.8
Hercules*	28.73, 36.87	132	187	-6.6	16.9 ± 0.7	17.9
Horologium I	271.38, -54.74	87	61	-3.5	...	18.2
Hydra II	295.62, 30.46	134	66	-4.8	...	17.8
Leo I	225.99, 49.11	254	223	-12.0	17.8 ± 0.2	17.3
Leo II*	220.17, 67.23	233	164	-9.8	18.0 ± 0.2	17.4
Leo IV*	265.44, 56.51	154	147	-5.8	16.3 ± 1.4	17.7
Leo V	261.86, 58.54	178	95	-5.2	16.4 ± 0.9	17.6
Pisces II	79.21, -47.11	182	45	-5.0	...	17.6
Reticulum II	266.30, -49.74	32	35	-3.6	18.9 ± 0.6	19.1
Sculptor*	287.53, -83.16	86	233	-11.1	18.5 ± 0.1	18.2
Segue 1*	220.48, 50.43	23	21	-1.5	19.4 ± 0.3	19.4
Sextans*	243.50, 42.27	86	561	-9.3	17.5 ± 0.2	18.2
Triangulum II	140.90, -23.82	30	30	-1.8	...	19.1
Tucana II	328.04, -52.35	58	120	-3.9	...	18.6
Ursa Major I	159.43, 54.41	97	143	-5.5	17.9 ± 0.5	18.1
Ursa Major II*	152.46, 37.44	32	91	-4.2	19.4 ± 0.4	19.1
Ursa Minor*	104.97, 44.80	76	120	-8.8	18.9 ± 0.2	18.3
Willman 1*	158.58, 56.78	38	19	-2.7	...	18.9
Likely Galaxies						
Columba I	231.62, -28.88	182	101	-4.5	...	17.6
Eridanus II	249.78, -51.65	331	156	-7.4	...	17.1
Grus I	338.68, -58.25	120	60	-3.4	...	17.9
Grus II	351.14, -51.94	53	93	-3.9	...	18.7
Horologium II	262.48, -54.14	78	33	-2.6	...	18.3
Indus II	354.00, -37.40	214	181	-4.3	...	17.4
Pegasus III	69.85, -41.81	205	57	-4.1	...	17.5
Phoenix II	323.69, -59.74	96	33	-3.7	...	18.1
Pictor I	257.29, -40.64	126	44	-3.7	...	17.9
Reticulum III	273.88, -45.65	92	64	-3.3	...	18.2
Sagittarius II	18.94, -22.90	67	34	-5.2	...	18.4
Tucana III	315.38, -56.18	25	44	-2.4	...	19.3
Tucana IV	313.29, -55.29	48	128	-3.5	...	18.7
Ambiguous Systems						
Cetus II	156.47, -78.53	30	17	0.0	...	19.1
Eridanus III	274.95, -59.60	96	12	-2.4	...	18.1
Kim 2	347.16, -42.07	105	12	-1.5	...	18.1
Tucana V	316.31, -51.89	55	16	-1.6	...	18.6

Fermi-LAT collaboration and DES collaboration [1611.03184]

DWARF GALAXY INDIRECT DETECTION CAVEATS

- Constraints rely on accurate J-factors

(1) Name	(2) l, b (deg, deg)	(3) Distance (kpc)	(4) $r_{1/2}$ (pc)	(5) M_V (mag)	(6) $\log_{10}(J_{\text{meas}})$ $\log_{10}(\text{GeV}^2 \text{cm}^{-5})$	(7) $\log_{10}(J_{\text{pred}})$ $\log_{10}(\text{GeV}^2 \text{cm}^{-5})$
Kinematically Confirmed Galaxies						
Boötes I*	358.08, 69.62	66	189	-6.3	18.2 ± 0.4	18.5
Boötes II	353.69, 68.87	42	46	-2.7	...	18.9
Boötes III	35.41, 75.35	47	...	-5.8	...	18.8
Canes Venatici I	74.31, 79.82	218	441	-8.6	17.4 ± 0.3	17.4
Canes Venatici II*	113.58, 82.70	160	52	-4.9	17.6 ± 0.4	17.7
Carina*	260.11, -22.22	105	205	-9.1	17.9 ± 0.1	18.1
Coma Berenices*	241.89, 83.61	44	60	-4.1	19.0 ± 0.4	18.8
Draco*	86.37, 34.72	76	184	-8.8	18.8 ± 0.1	18.3
Draco II	98.29, 42.88	24	16	-2.9	...	19.3
Fornax*	237.10, -65.65	147	594	-13.4	17.8 ± 0.1	17.8
Hercules*	28.73, 36.87	132	187	-6.6	16.9 ± 0.7	17.9
Horologium I	271.38, -54.74	87	61	-3.5	...	18.2
Hydra II	295.62, 30.46	134	66	-4.8	...	17.8
Leo I	225.99, 49.11	254	223	-12.0	17.8 ± 0.2	17.3
Leo II*	220.17, 67.23	233	164	-9.8	18.0 ± 0.2	17.4
Leo IV*	265.44, 56.51	154	147	-5.8	16.3 ± 1.4	17.7
Leo V	261.86, 58.54	178	95	-5.2	16.4 ± 0.9	17.6
Pisces II	79.21, -47.11	182	45	-5.0	...	17.6
Reticulum II	266.30, -49.74	32	35	-3.6	18.9 ± 0.6	19.1
Sculptor*	287.53, -83.16	86	233	-11.1	18.5 ± 0.1	18.2
Segue 1*	220.48, 50.43	23	21	-1.5	19.4 ± 0.3	19.4
Sextans*	243.50, 42.27	86	561	-9.3	17.5 ± 0.2	18.2
Triangulum II	140.90, -23.82	30	30	-1.8	...	19.1
Tucana II	328.04, -52.35	58	120	-3.9	...	18.6
Ursa Major I	159.43, 54.41	97	143	-5.5	17.9 ± 0.5	18.1
Ursa Major II*	152.46, 37.44	32	91	-4.2	19.4 ± 0.4	19.1
Ursa Minor*	104.97, 44.80	76	120	-8.8	18.9 ± 0.2	18.3
Willman 1*	158.58, 56.78	38	19	-2.7	...	18.9
Likely Galaxies						
Columba I	231.62, -28.88	182	101	-4.5	...	17.6
Eridanus II	249.78, -51.65	331	156	-7.4	...	17.1
Grus I	338.68, -58.25	120	60	-3.4	...	17.9
Grus II	351.14, -51.94	53	93	-3.9	...	18.7
Horologium II	262.48, -54.14	78	33	-2.6	...	18.3
Indus II	354.00, -37.40	214	181	-4.3	...	17.4
Pegasus III	69.85, -41.81	205	57	-4.1	...	17.5
Phoenix II	323.69, -59.74	96	33	-3.7	...	18.1
Pictor I	257.29, -40.64	126	44	-3.7	...	17.9
Reticulum III	273.88, -45.65	92	64	-3.3	...	18.2
Sagittarius II	18.94, -22.90	67	34	-5.2	...	18.4
Tucana III	315.38, -56.18	25	44	-2.4	...	19.3
Tucana IV	313.29, -55.29	48	128	-3.5	...	18.7
Ambiguous Systems						
Cetus II	156.47, -78.53	30	17	0.0	...	19.1
Eridanus III	274.95, -59.60	96	12	-2.4	...	18.1
Kim 2	347.16, -42.07	105	12	-1.5	...	18.1
Tucana V	316.31, -51.89	55	16	-1.6	...	18.6

Use with caution:

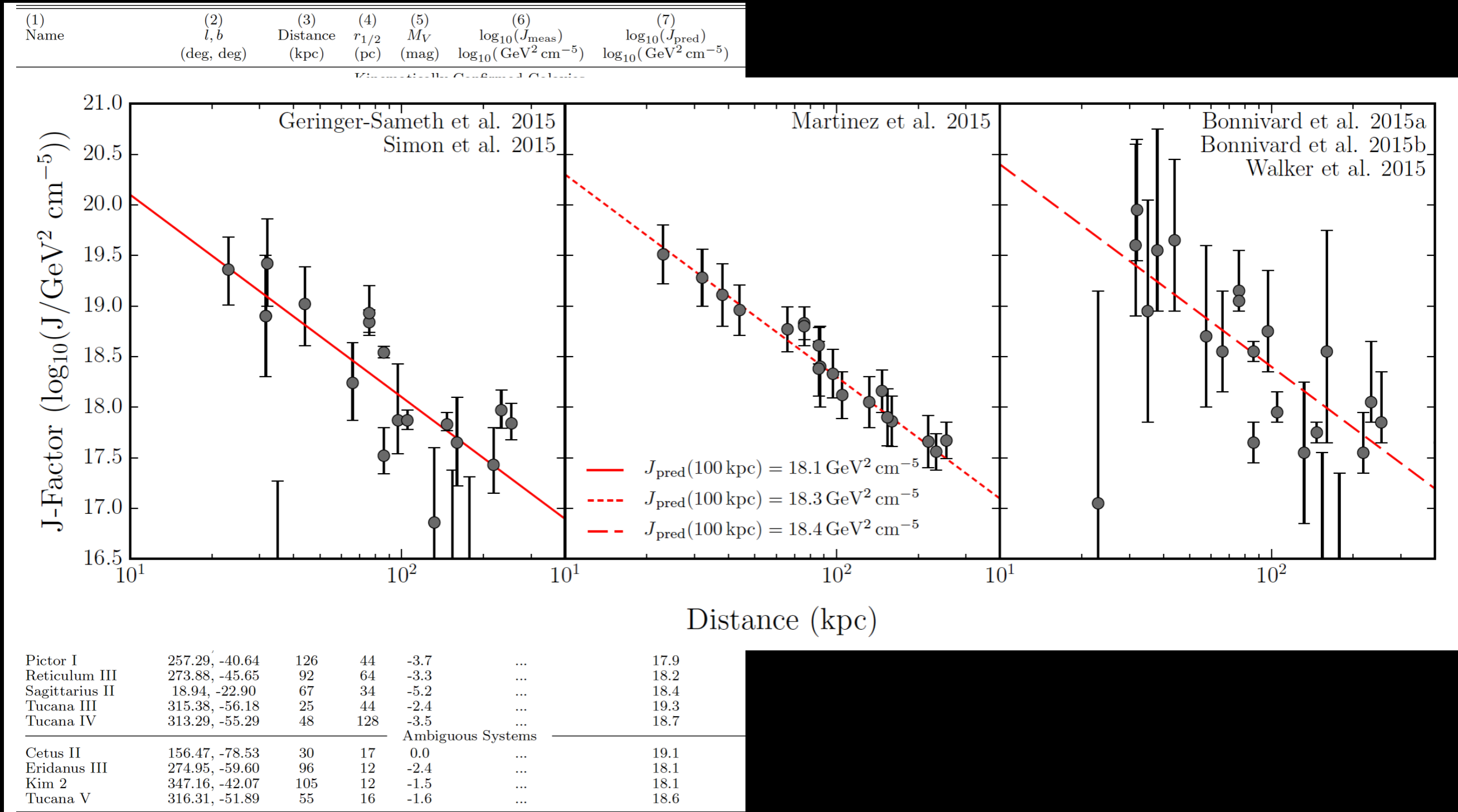
“Galaxies for which Published Kinematics May Not Reliably Translate to Masses”

J. D. Simon [1901.05465]

Fermi-LAT collaboration and DES collaboration [1611.03184]

DWARF GALAXY INDIRECT DETECTION CAVEATS

- Constraints rely on accurate J-factors



Fermi-LAT collaboration and DES collaboration [1611.03184]

INFERRING DWARF GALAXY J-FACTORS

INFERRING DWARF GALAXY J-FACTORS

- Important assumptions:

INFERRING DWARF GALAXY J-FACTORS

- Important assumptions:
 - Equilibrium
K. El-Badry et al. [1610.04232]

INFERRING DWARF GALAXY J-FACTORS

- Important assumptions:
 - Equilibrium
K. El-Badry et al. [1610.04232]
 - Spherical system
V. Bonnivard et al. [1407.7822]

INFERRING DWARF GALAXY J-FACTORS

- Important assumptions:
 - Equilibrium
K. El-Badry et al. [1610.04232]
 - Spherical system
V. Bonnivard et al. [1407.7822]
 - Non-rotating system

INFERRING DWARF GALAXY J-FACTORS

- Important assumptions:

- Equilibrium

K. El-Badry et al. [1610.04232]

- Spherical system

V. Bonnivard et al. [1407.7822]

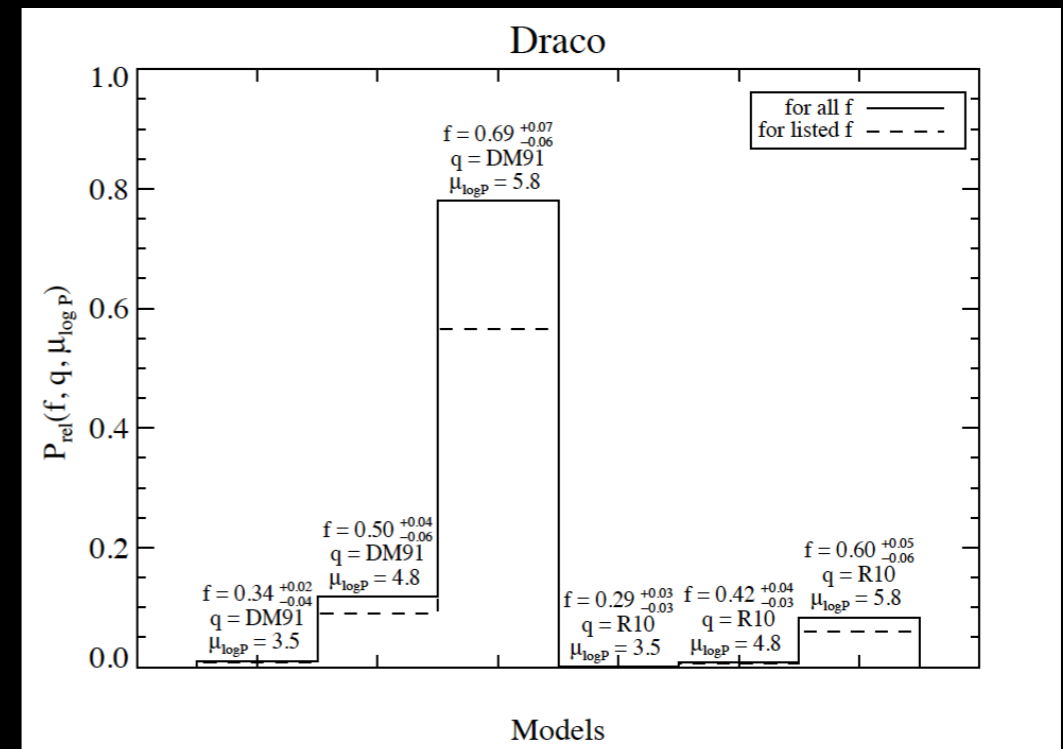
- Non-rotating system

- **No accounting for binaries**

A. W. McConnachie and P. Cote [1009.4205]

M. E. Spencer et al. [1811.06597]

M. E. Spencer et al. [1706.04184]



M. E. Spencer et al. [1811.06597]

INFERRING DWARF GALAXY J-FACTORS

- Important assumptions:

- Equilibrium

K. El-Badry et al. [1610.04232]

- Spherical system

V. Bonnivard et al. [1407.7822]

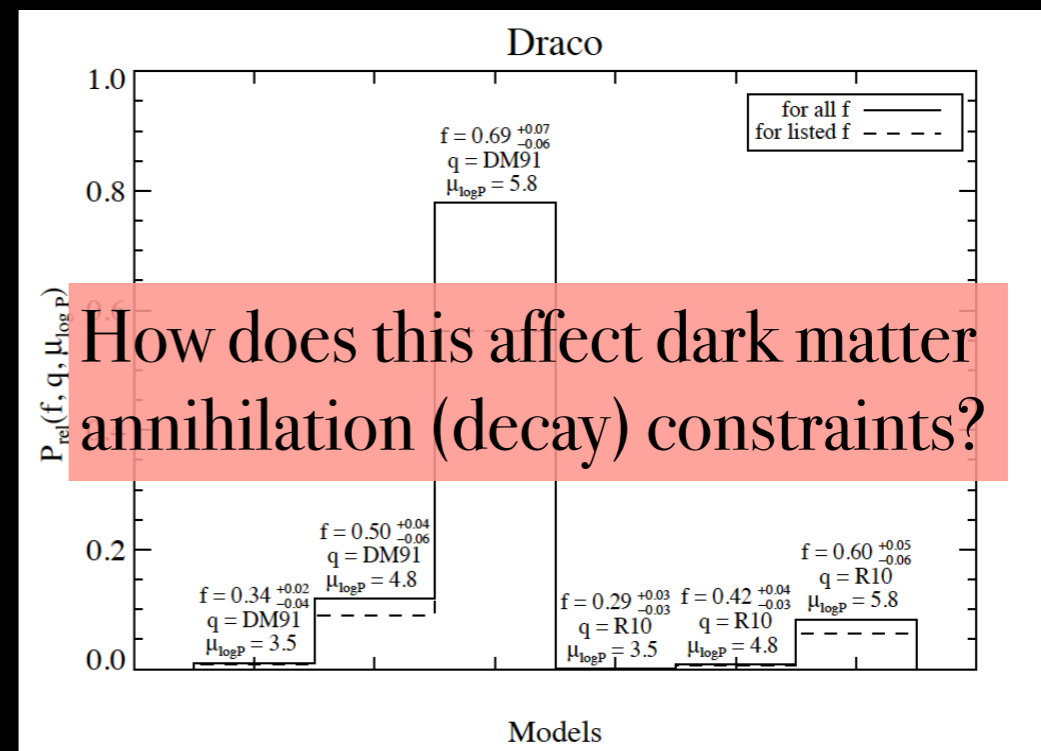
- Non-rotating system

- **No accounting for binaries**

A. W. McConnachie and P. Cote [1009.4205]

M. E. Spencer et al. [1811.06597]

M. E. Spencer et al. [1706.04184]



M. E. Spencer et al. [1811.06597]

INFERRING DWARF GALAXY J-FACTORS

- Important assumptions:

- Equilibrium

K. El-Badry et al. [1610.04232]

- Spherical system

V. Bonnivard et al. [1407.7822]

- Non-rotating system

- **No accounting for binaries**

A. W. McConnachie and P. Cote [1009.4205]

M. E. Spencer et al. [1811.06597]

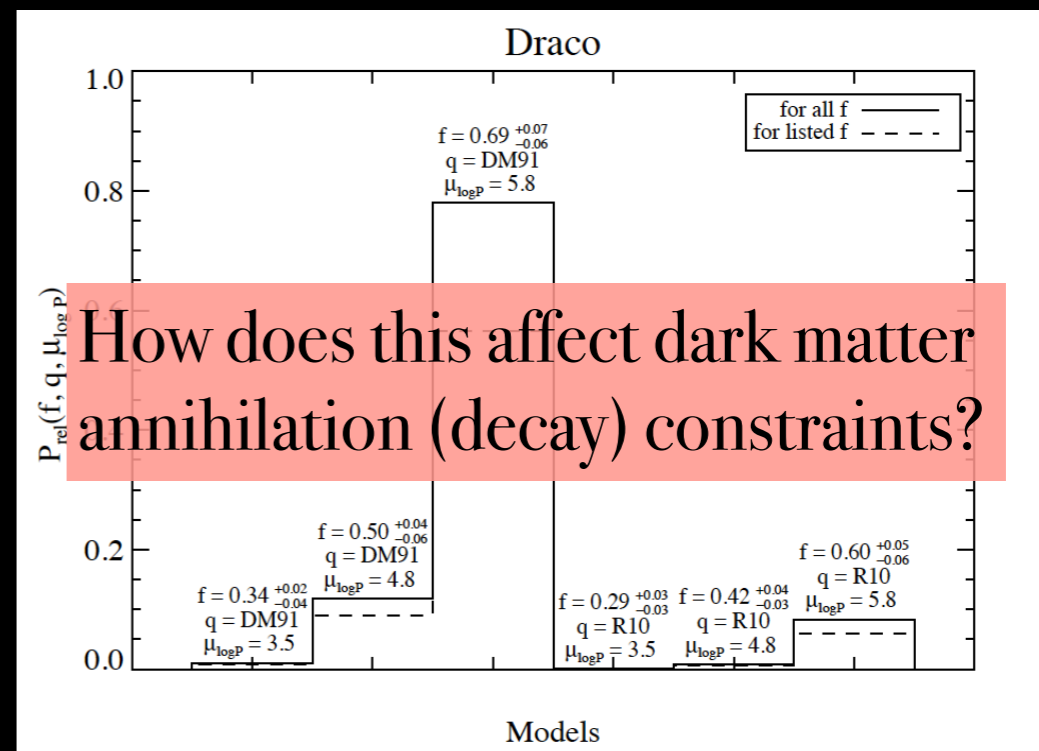
M. E. Spencer et al. [1706.04184]

Spherical Jeans equation

3d radial velocity dispersion,
stellar density profile



Halo mass (DM density profile)



M. E. Spencer et al. [1811.06597]

INFERRING DWARF GALAXY J-FACTORS

- Important assumptions:

- Equilibrium

K. El-Badry et al. [1610.04232]

- Spherical system

V. Bonnivard et al. [1407.7822]

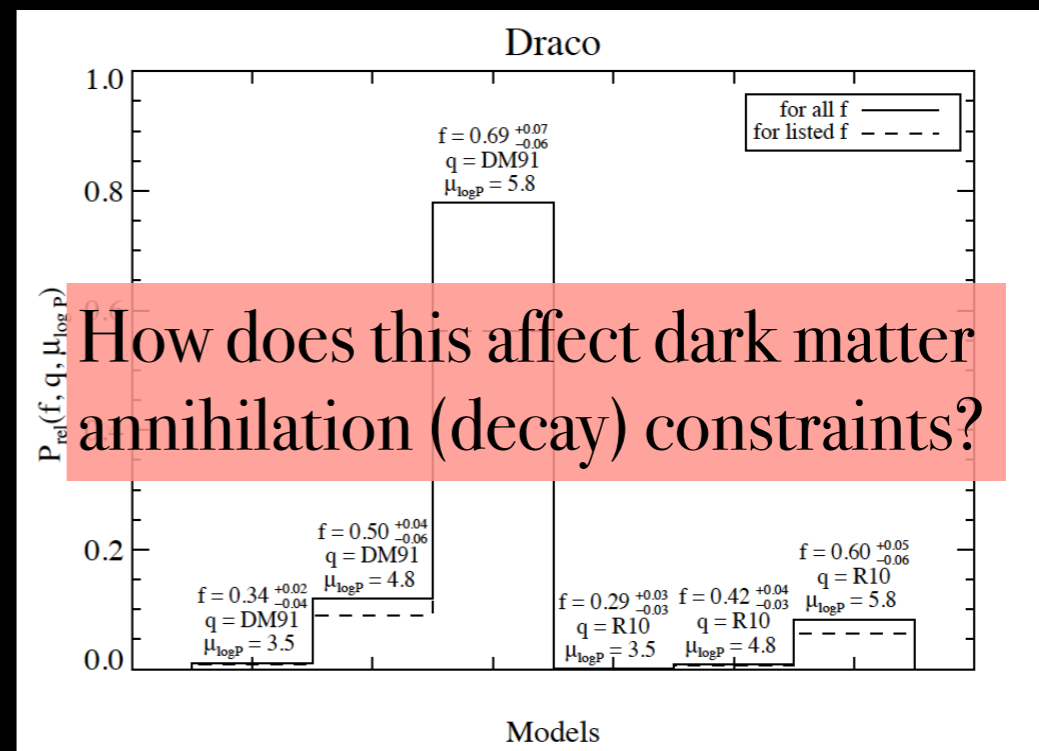
- Non-rotating system

- **No accounting for binaries**

A. W. McConnachie and P. Cote [1009.4205]

M. E. Spencer et al. [1811.06597]

M. E. Spencer et al. [1706.04184]



M. E. Spencer et al. [1811.06597]

In practice, observe line-of-sight projected quantities

Line-of-sight projected
velocity dispersion,
stellar density profile

$M - \beta (\rho - \beta)$ degeneracy

J.I. Read and P. Steger [1701.04833]



Halo mass (DM density profile)



J-factor \longrightarrow
(+ particle physics)

Constraint on
DM annihilation

OUTLINE OF METHODOLOGY

OUTLINE OF METHODOLOGY

The question

OUTLINE OF METHODOLOGY

The question

In the cleanest scenario, what is the effect of binaries on dwarf galaxy J-factors?

OUTLINE OF METHODOLOGY

The question

In the cleanest scenario, what is the effect of binaries on dwarf galaxy J-factors?

The (simulated) data

OUTLINE OF METHODOLOGY

The question

In the cleanest scenario, what is the effect of binaries on dwarf galaxy J-factors?

The (simulated) data

Gaia Challenge spherical mocks:

- Plummer light profile
- Cusped DM profile
- No velocity anisotropy

Gaia Challenge <http://astrowiki.ph.surrey.ac.uk/dokuwiki>
M. G. Walker and J. Peñarrubia [1108.2404]

OUTLINE OF METHODOLOGY

The question

In the cleanest scenario, what is the effect of binaries on dwarf galaxy J-factors?

The (simulated) data

Gaia Challenge spherical mocks:

- Plummer light profile
- Cusped DM profile
- No velocity anisotropy

Gaia Challenge <http://astrowiki.ph.surrey.ac.uk/dokuwiki>
M. G. Walker and J. Peñarrubia [1108.2404]

The model

OUTLINE OF METHODOLOGY

The question

In the cleanest scenario, what is the effect of binaries on dwarf galaxy J-factors?

The (simulated) data

Gaia Challenge spherical mocks:

Gaia Challenge <http://astrowiki.ph.surrey.ac.uk/dokuwiki>
M. G. Walker and J. Peñarrubia [1108.2404]

- Plummer light profile
- Cusped DM profile
- No velocity anisotropy

The model

J.I. Read and P. Steger [1701.04833]

- Nested Plummer light profile: sum of 2 Plummer, independent norm & scale
- Broken power law DM profile: spans cusped \leftrightarrow cored

OUTLINE OF METHODOLOGY

The question

In the cleanest scenario, what is the effect of binaries on dwarf galaxy J-factors?

The (simulated) data

Gaia Challenge spherical mocks:

Gaia Challenge <http://astrowiki.ph.surrey.ac.uk/dokuwiki>
M. G. Walker and J. Peñarrubia [1108.2404]

- Plummer light profile
- Cusped DM profile
- No velocity anisotropy

The model

J.I. Read and P. Steger [1701.04833]

- Nested Plummer light profile: sum of 2 Plummer, independent norm & scale
- Broken power law DM profile: spans cusped \leftrightarrow cored

The method

OUTLINE OF METHODOLOGY

The question

In the cleanest scenario, what is the effect of binaries on dwarf galaxy J-factors?

The (simulated) data

Gaia Challenge spherical mocks:

Gaia Challenge <http://astrowiki.ph.surrey.ac.uk/dokuwiki>
M. G. Walker and J. Peñarrubia [1108.2404]

- Plummer light profile
- Cusped DM profile
- No velocity anisotropy

The model

J.I. Read and P. Steger [1701.04833]

- Nested Plummer light profile: sum of 2 Plummer, independent norm & scale
- Broken power law DM profile: spans cusped \leftrightarrow cored

The method

Run through pipeline to get J-factors for Gaia Challenge

OUTLINE OF METHODOLOGY

The question

In the cleanest scenario, what is the effect of binaries on dwarf galaxy J-factors?

The (simulated) data

Gaia Challenge spherical mocks:

Gaia Challenge <http://astrowiki.ph.surrey.ac.uk/dokuwiki>
M. G. Walker and J. Peñarrubia [1108.2404]

- Plummer light profile
- Cusped DM profile
- No velocity anisotropy

The model

J.I. Read and P. Steger [1701.04833]

- Nested Plummer light profile: sum of 2 Plummer, independent norm & scale
- Broken power law DM profile: spans cusped \leftrightarrow cored

The method

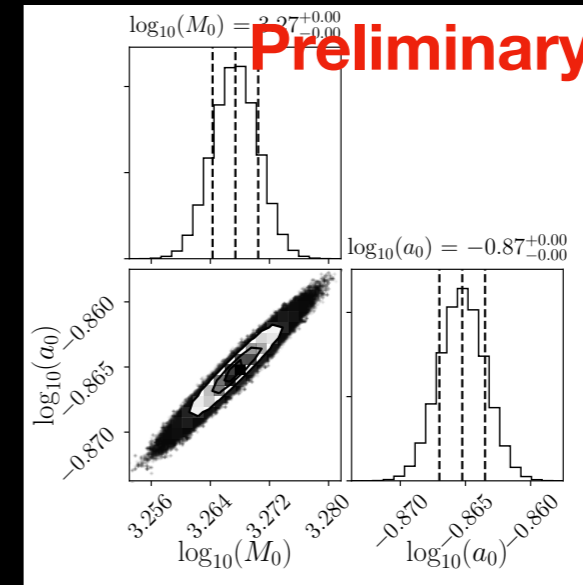
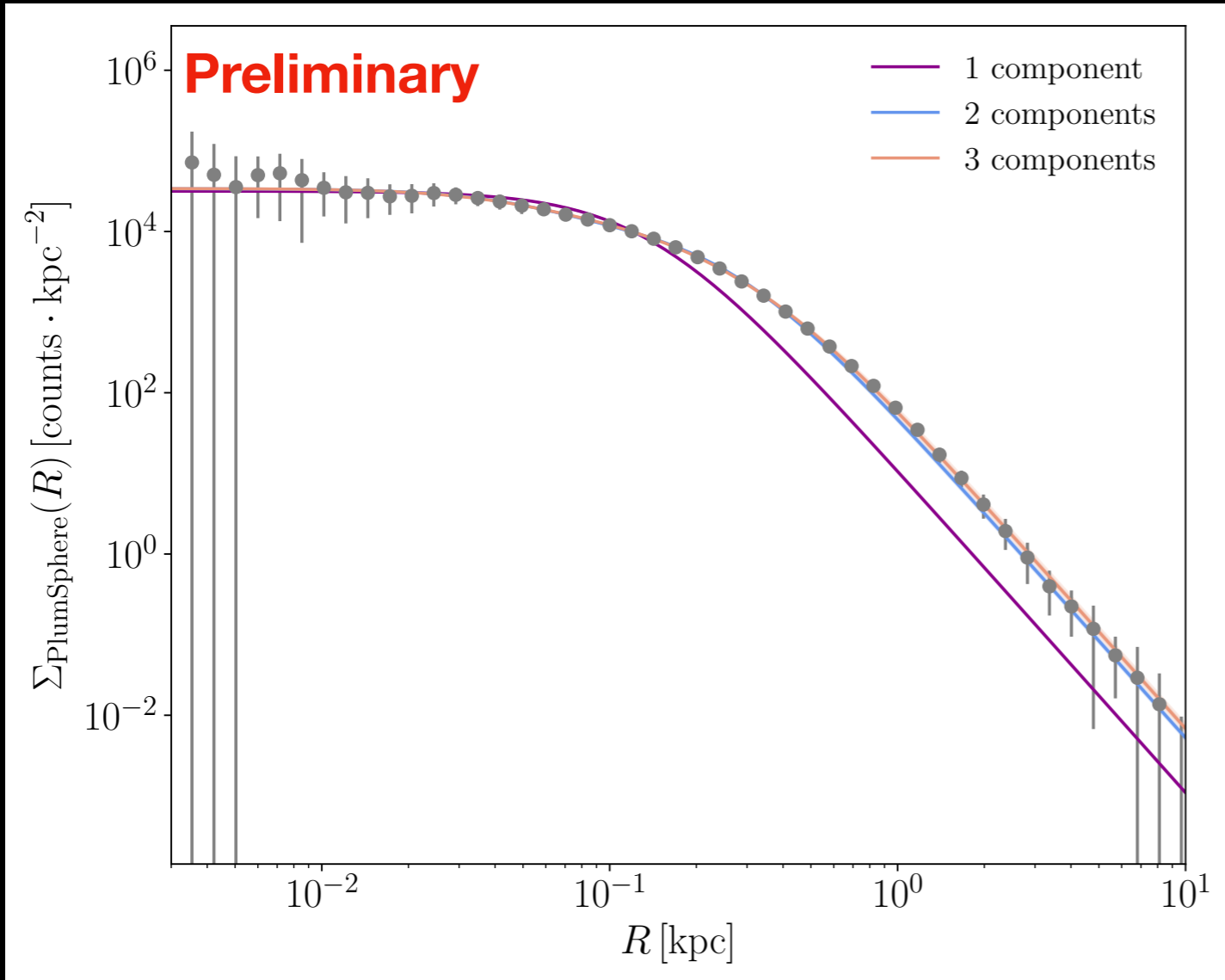
Run through pipeline to get J-factors for Gaia Challenge

→ Repeat analysis with injected binary motions

STEP 1: LIGHT PROFILE FIT

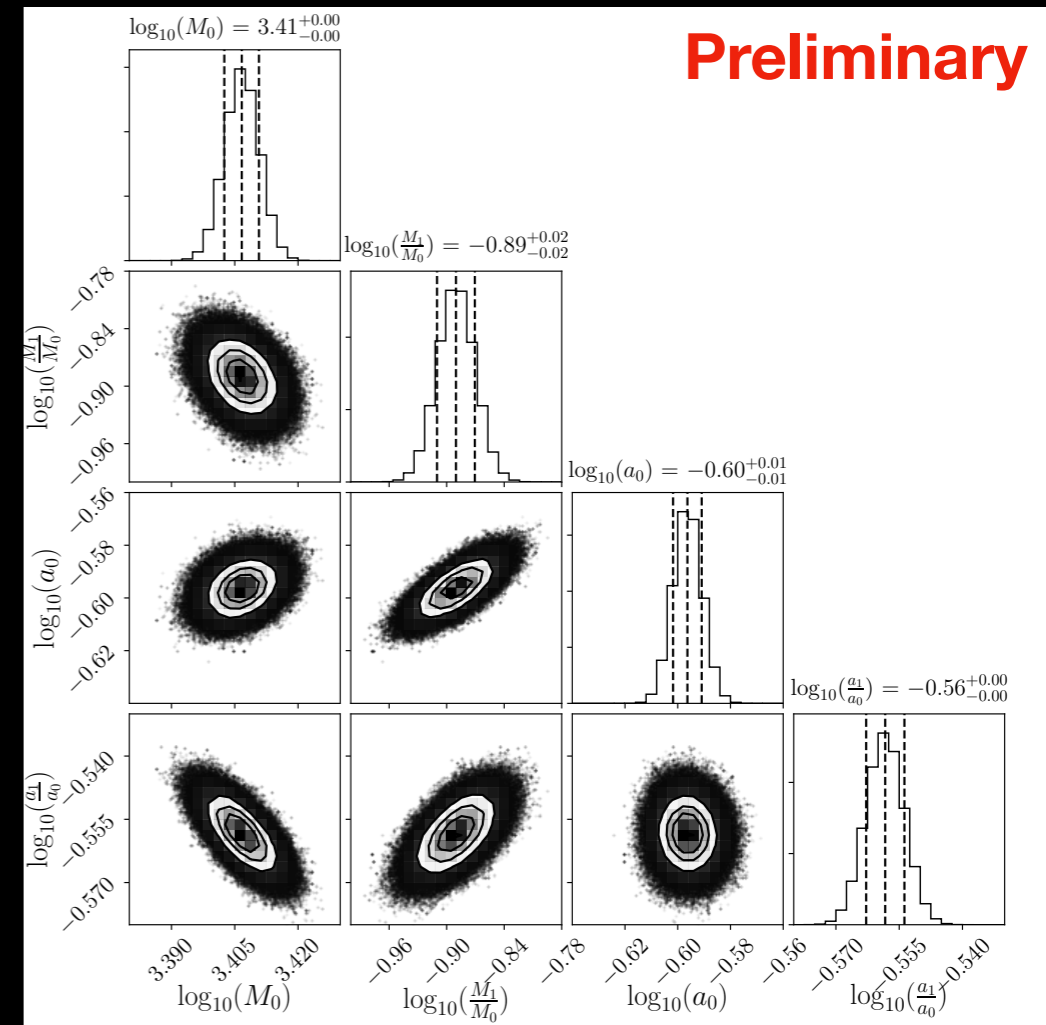
- Binned likelihood fit to stellar positions
- Fits tend to be well-constrained

3000 tracers



1 Plummer component

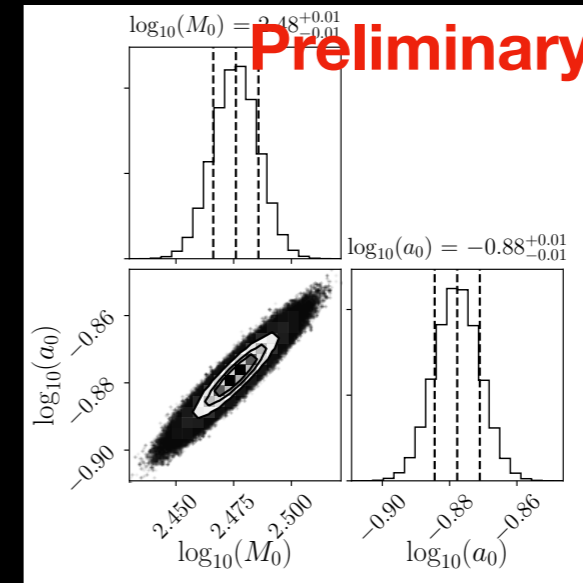
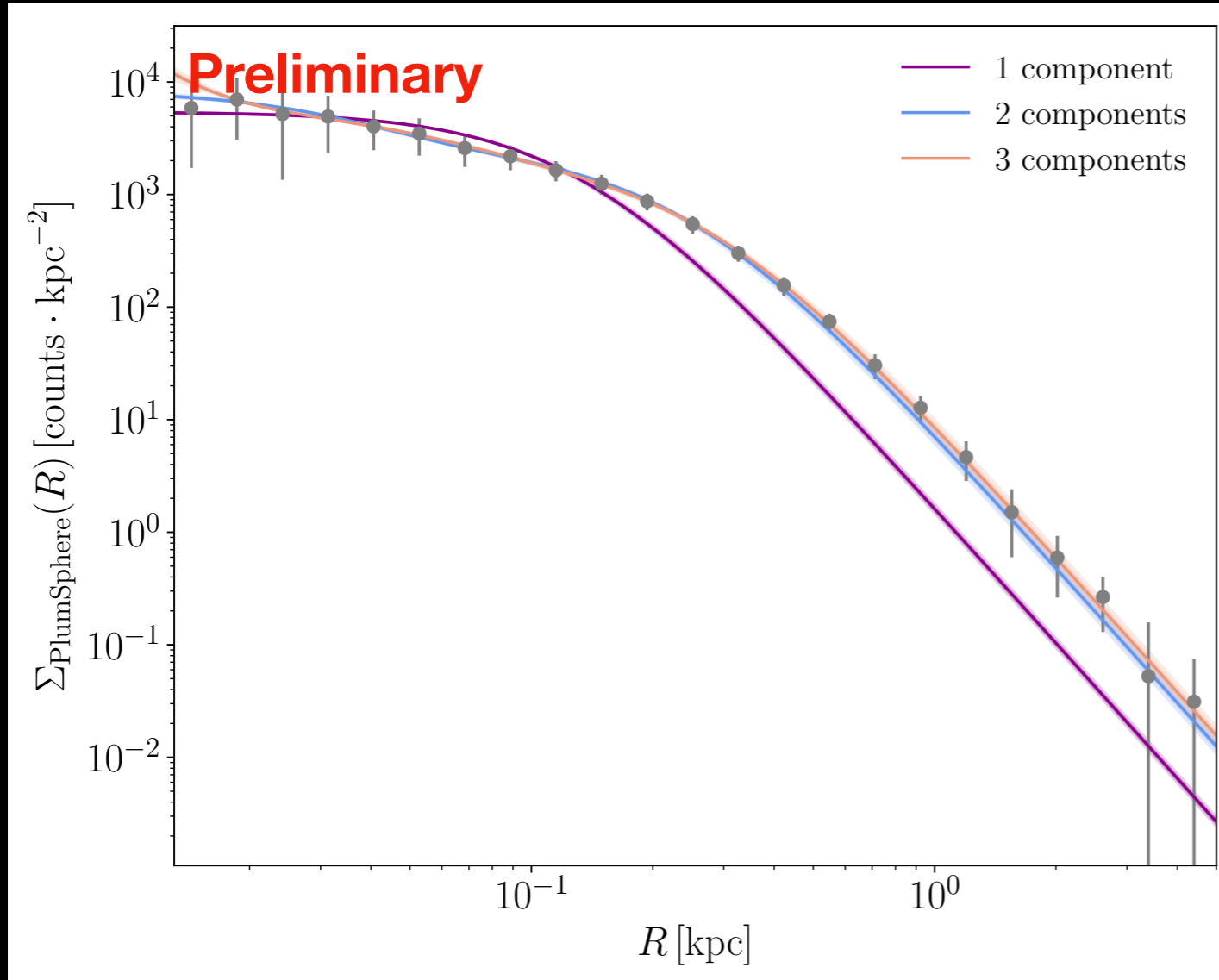
2 Plummer components



STEP 1: LIGHT PROFILE FIT

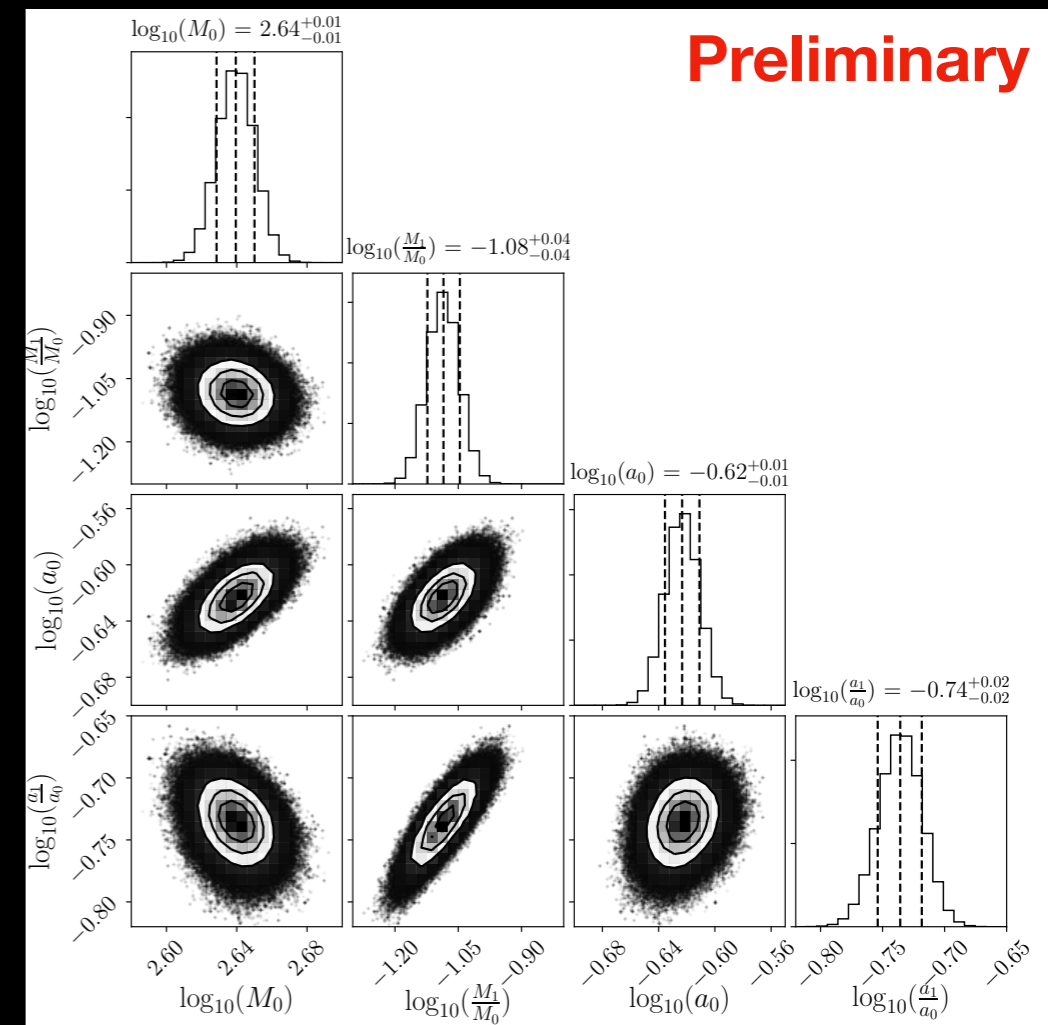
- Binned likelihood fit to stellar positions
- Fits tend to be well-constrained

500 tracers



← 1 Plummer component

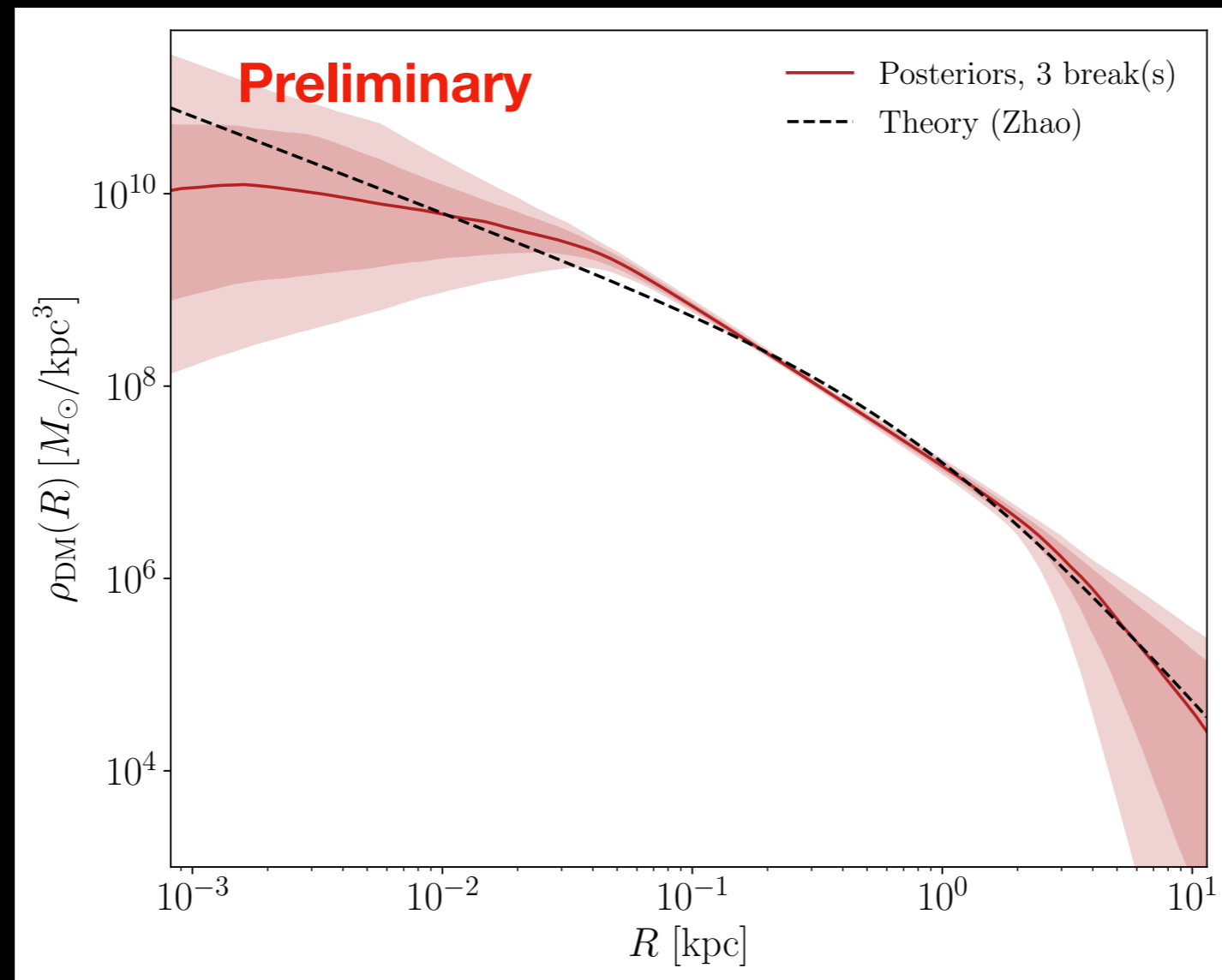
2 Plummer components



STEP 2: VELOCITY DISPERSION FIT

- Use Step 1 to constrain light profile parameters: float over middle 95% posterior parameter ranges from light profile fit
- Optimistically assume velocity error of 0.2 km/s
- Extract posterior distributions for DM parameters

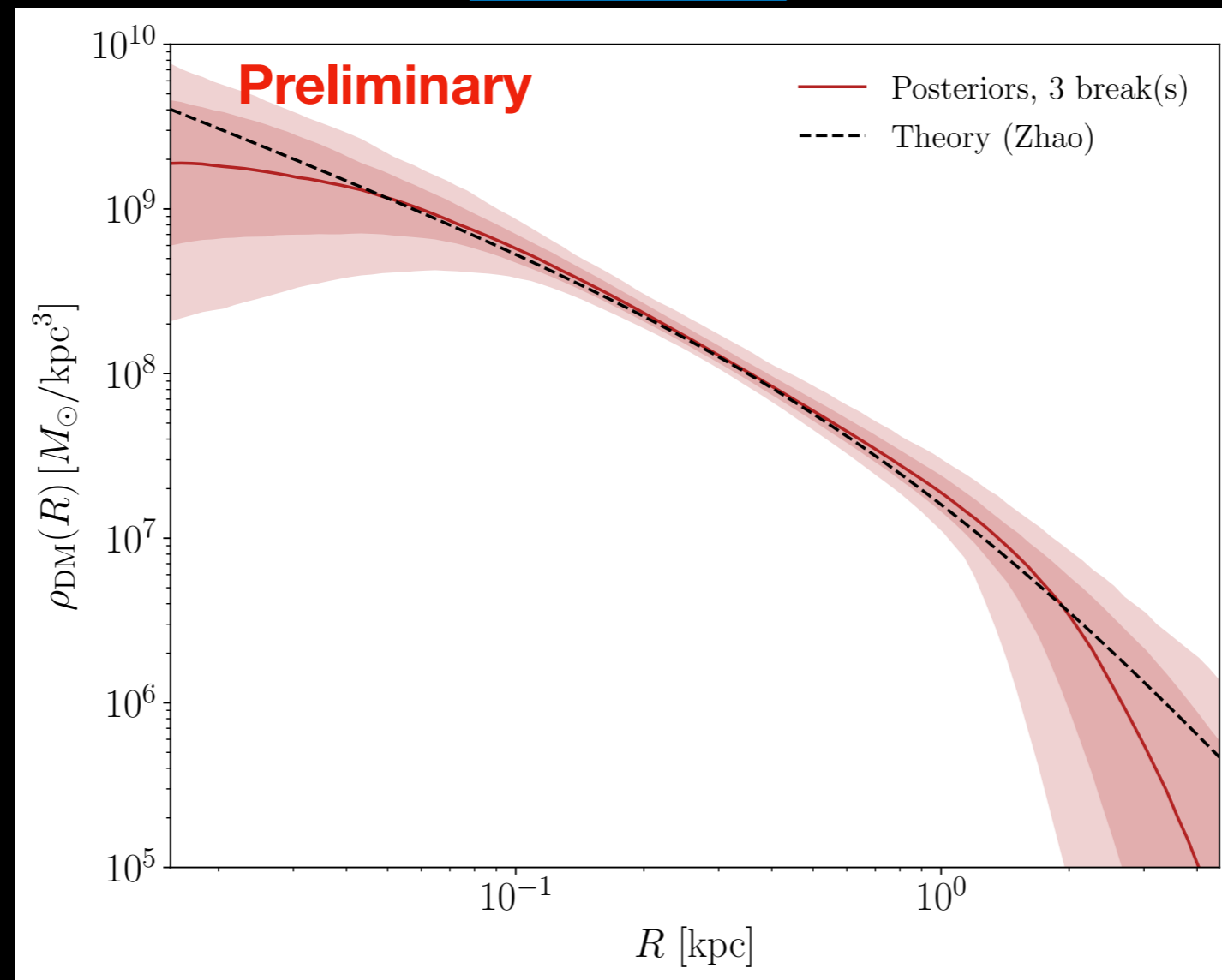
3000 tracers



STEP 2: VELOCITY DISPERSION FIT

- Use Step 1 to constrain light profile parameters: float over middle 95% posterior parameter ranges from light profile fit
- Optimistically assume velocity error of 0.2 km/s
- Extract posterior distributions for DM parameters

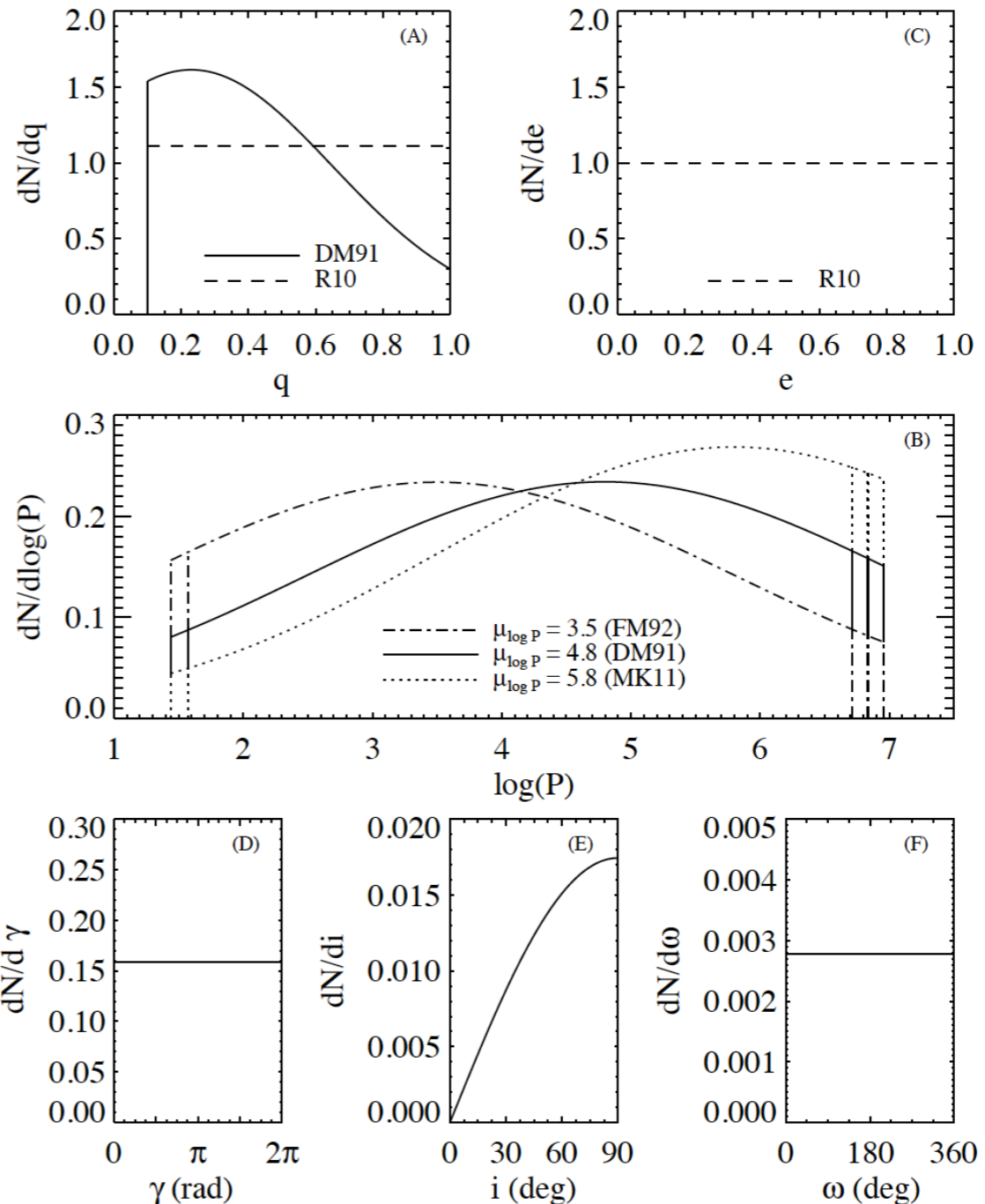
500 tracers



INJECTING BINARIES

M. E. Spencer et al. [1811.06597]

$$v_{r,orb} = \frac{q \sin i}{\sqrt{1-e^2}} \left(\frac{2\pi G m_1}{P(1+q)^2} \right)^{1/3} (\cos(\theta + \omega) + e \cos \omega). \quad (2)$$

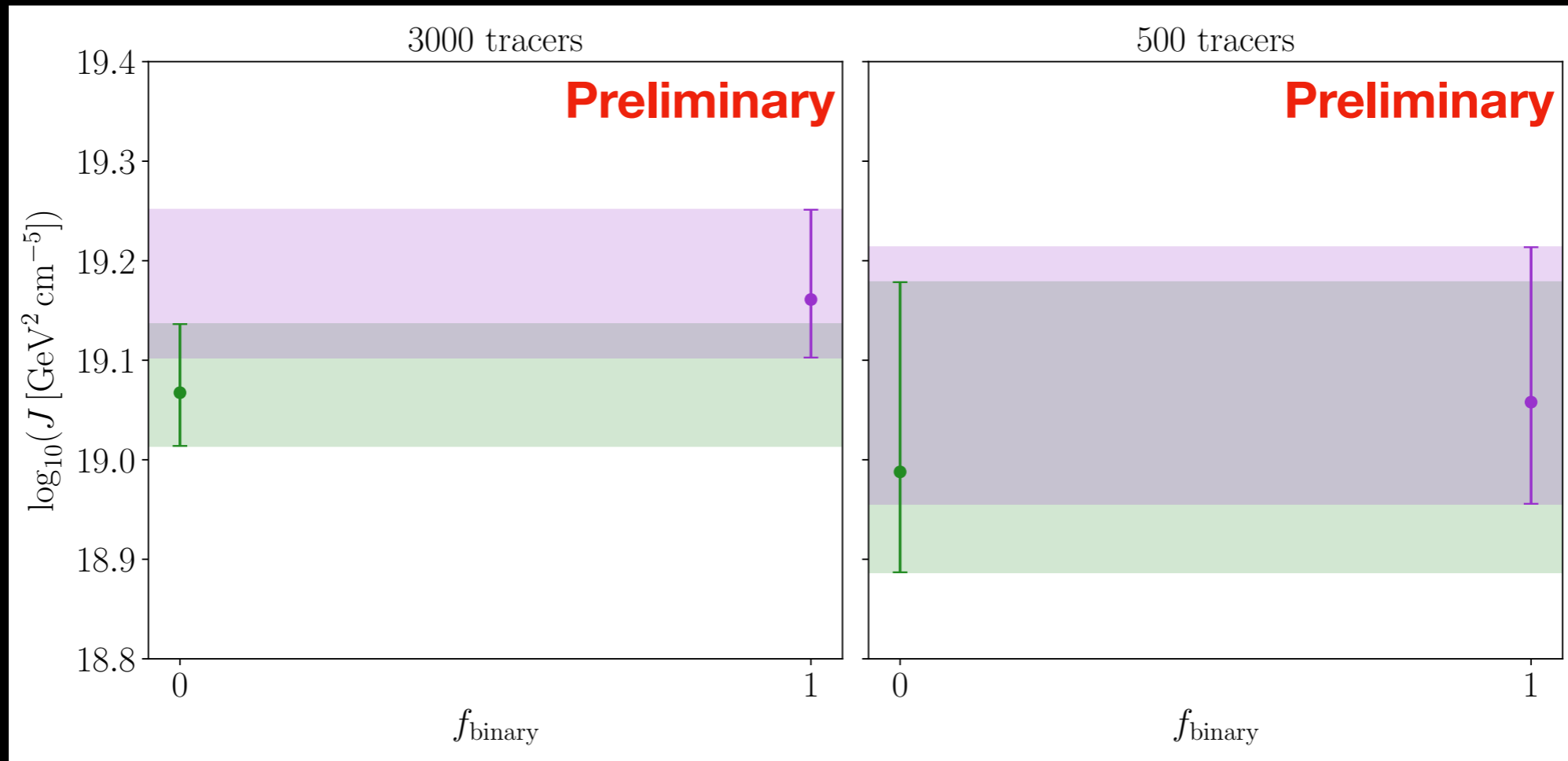


As a starting point:

Model and code for modeling binary motion from Spencer+ 2018

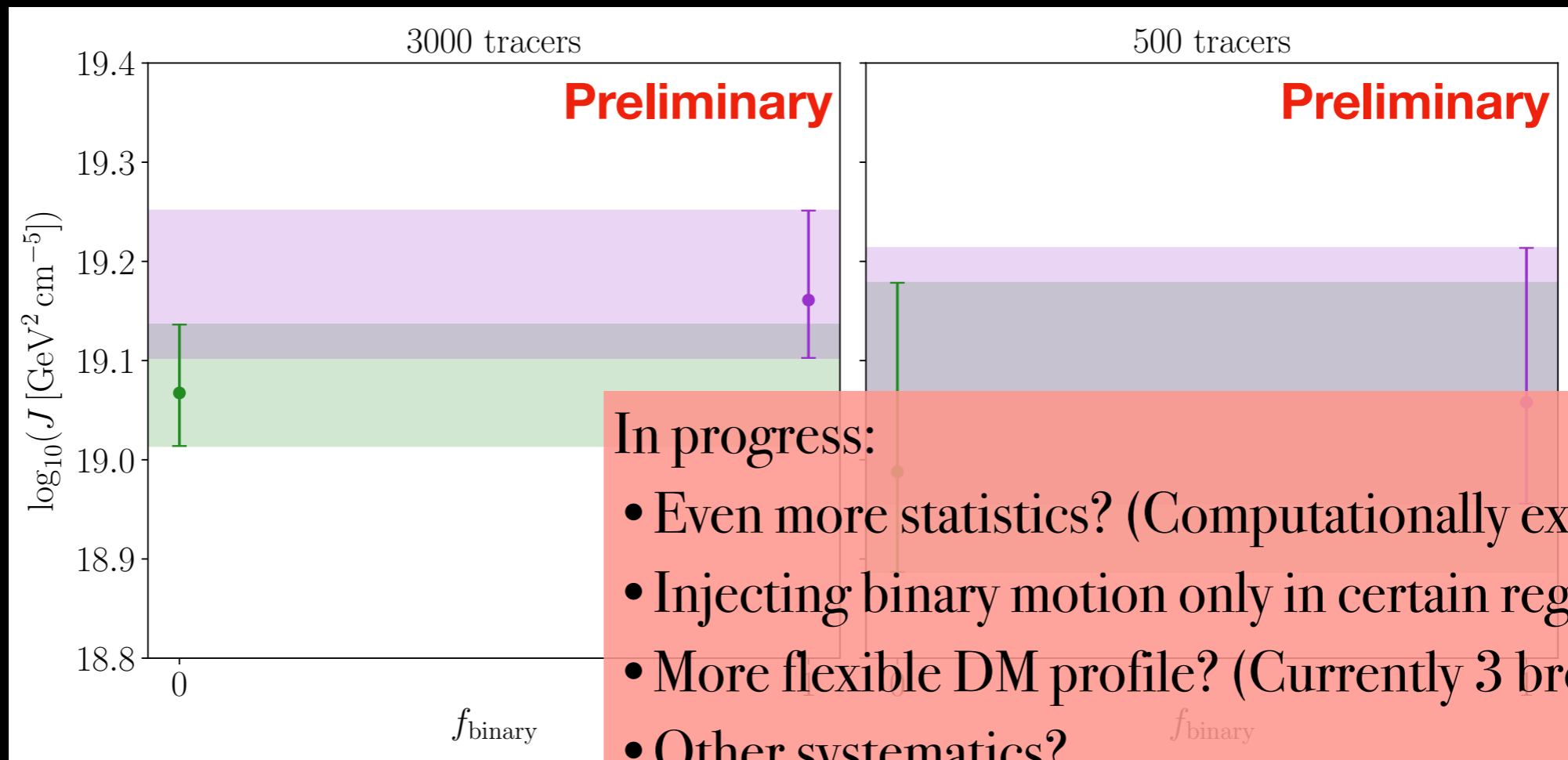
(If you have a favorite binary model we should try, please let us know!)

EFFECT OF UNMODELED BINARIES ON J-FACTORS



N_{tracers}	f_{binary}	$\log_{10}(M(<R_{1/2})/M_{\odot})$	$\log_{10}(M(<R_{\text{max}})/M_{\odot})$	$\log_{10}(J/(\text{GeV}^2 \text{cm}^{-5}))$
3000	0	$7.32^{+0.02}_{-0.02}$	$9.14^{+0.25}_{-0.26}$	$19.07^{+0.07}_{-0.05}$
3000	1	$7.38^{+0.17}_{-0.19}$	$9.19^{+0.23}_{-0.20}$	$19.16^{+0.09}_{-0.06}$
500	0	$7.25^{+0.04}_{-0.05}$	$8.81^{+0.18}_{-0.17}$	$18.99^{+0.19}_{-0.10}$
500	1	$7.30^{+0.04}_{-0.04}$	$8.76^{+0.21}_{-0.18}$	$19.06^{+0.16}_{-0.10}$

EFFECT OF UNMODELED BINARIES ON J-FACTORS



N_{tracers}	f_{binary}	$\log_{10}(M(<R_{1/2})/M_{\odot})$	$\log_{10}(M(<R_{\text{max}})/M_{\odot})$	$\log_{10}(J/(\text{GeV}^2 \text{cm}^{-5}))$
3000	0	$7.32^{+0.02}_{-0.02}$	$9.14^{+0.25}_{-0.26}$	$19.07^{+0.07}_{-0.05}$
3000	1	$7.38^{+0.17}_{-0.19}$	$9.19^{+0.23}_{-0.20}$	$19.16^{+0.09}_{-0.06}$
500	0	$7.25^{+0.04}_{-0.05}$	$8.81^{+0.18}_{-0.17}$	$18.99^{+0.19}_{-0.10}$
500	1	$7.30^{+0.04}_{-0.04}$	$8.76^{+0.21}_{-0.18}$	$19.06^{+0.16}_{-0.10}$

CONCLUSIONS & EXTENSIONS

- In very simple examples on mock data, the presence of unmodeled binaries can bias estimates of dwarf galaxy J-factors \Rightarrow bias dark matter constraints derived
- Effect of binaries becomes more drastic with increased statistics
 - With more stars measured and more accurate measurements, will this become a more measurable effect? [J. D. Simon et al. \[1903.04743\]](#)
 - With future multi-epoch binary measurements, could exclude confirmed binaries from analysis
- Statistical uncertainties in dwarf galaxy dark matter constraints need to be better understood and characterized
- Other important systematics: tidal disruption, deviations from equilibrium, non-sphericity, ...

BACKUP SLIDES

INDIRECT DETECTION BENCHMARK: DWARF GALAXIES

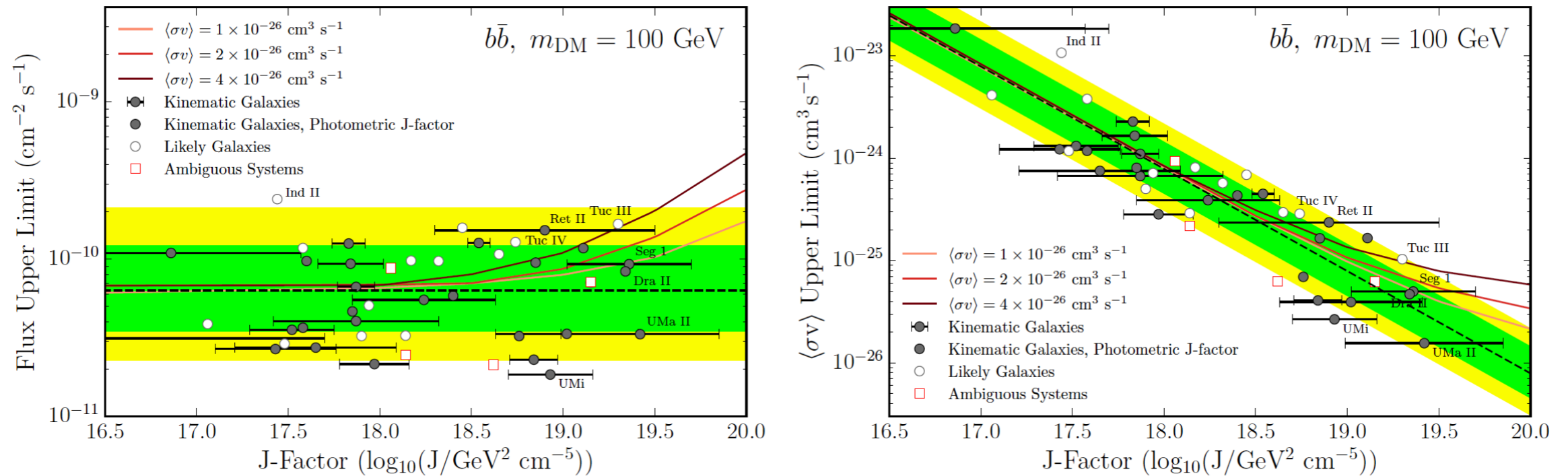


Figure 6. Upper limits on flux (*left*) and cross section (*right*) versus J-factor. The points represent J-factors for each target estimated either from spectroscopy (filled circles with error bars) or from the scaling relation discussed in Section 4 (filled circles). The green and yellow shaded regions are the 68% and 95% containment regions for the blank-sky expectations, respectively. For comparison, the three solid lines show the median expected upper limits for DM annihilation with the given cross section. No significant deviation from the background-only expectation is observed.

INFERRING DWARF GALAXY J-FACTORS

$$\frac{1}{\nu} \frac{d}{dr} (\nu \bar{v}_r^2) + 2 \frac{\beta_{\text{ani}} \bar{v}_r^2}{r} = - \frac{GM(r)}{r^2}$$

3d radial velocity dispersion

velocity anisotropy

$$M(r) \approx 4\pi \int_0^r \rho_{\text{DM}}(r') r'^2 dr'$$

INFERRING DWARF GALAXY J-FACTORS

Spherical Jeans equation

$$\frac{1}{\nu} \frac{d}{dr} (\nu \bar{v}_r^2) + 2 \frac{\beta_{\text{ani}} \bar{v}_r^2}{r} = - \frac{GM(r)}{r^2}$$

3d radial velocity dispersion
velocity anisotropy
 $M(r) \approx 4\pi \int_0^r \rho_{\text{DM}}(r') r'^2 dr'$

In practice, observe line-of-sight projected quantities

$$\sigma_p^2(R) = \frac{2}{\Sigma(R)} \int_R^\infty \left(1 - \beta_{\text{ani}}(r) \frac{R^2}{r^2} \right) \nu(r) \bar{v}_r^2(r) \frac{r dr}{\sqrt{r^2 - R^2}}$$

INFERRING DWARF GALAXY J-FACTORS

Spherical Jeans equation

$$\frac{1}{\nu} \frac{d}{dr} (\nu \bar{v}_r^2) + 2 \frac{\beta_{\text{ani}} \bar{v}_r^2}{r} = - \frac{GM(r)}{r^2}$$

$\nu \bar{v}_r^2$ → 3d radial velocity dispersion
 $\beta_{\text{ani}} \bar{v}_r^2$ → velocity anisotropy
 $M(r) \approx 4\pi \int_0^r \rho_{\text{DM}}(r') r'^2 dr'$

In practice, observe line-of-sight projected quantities

$$\sigma_p^2(R) = \frac{2}{\Sigma(R)} \int_R^\infty \left(1 - \beta_{\text{ani}}(r) \frac{R^2}{r^2} \right) \nu(r) \bar{v}_r^2(r) \frac{r dr}{\sqrt{r^2 - R^2}}$$

$\sigma_p^2(R)$ → projected velocity dispersion

INFERRING DWARF GALAXY J-FACTORS

Spherical Jeans equation

$$\frac{1}{\nu} \frac{d}{dr} (\nu \bar{v}_r^2) + 2 \frac{\beta_{\text{ani}} \bar{v}_r^2}{r} = - \frac{GM(r)}{r^2}$$

$\nu \bar{v}_r^2$ → 3d radial velocity dispersion
 $\beta_{\text{ani}} \bar{v}_r^2$ → velocity anisotropy
 $M(r) \approx 4\pi \int_0^r \rho_{\text{DM}}(r') r'^2 dr'$

In practice, observe line-of-sight projected quantities

$$\sigma_p^2(R) = \frac{2}{\Sigma(R)} \int_R^\infty \left(1 - \beta_{\text{ani}}(r) \frac{R^2}{r^2} \right) \nu(r) \bar{v}_r^2(r) \frac{r dr}{\sqrt{r^2 - R^2}}$$

$\sigma_p^2(R)$ → projected velocity dispersion
 $\Sigma(R)$ → 2d stellar density ("light profile")

FIDUCIAL SETUP

- Nested Plummer light profile

J.I. Read and P. Steger [1701.04833]

$$\nu(r) = \sum_{i=1}^{N_p} \frac{3M_i}{4\pi a_i^3} \times \left(1 + \frac{r^2}{a_i^2}\right)^{-5/2} \xleftrightarrow{\text{Abel transform}} \Sigma(R) = \sum_{i=1}^{N_p} \frac{M_i a_i^2}{\pi(a_i^2 + R^2)^2}$$

- Broken power law DM profile: analytic formula for enclosed DM mass

$$\rho(r) = \begin{cases} \rho_0 \left(\frac{r}{r_0}\right)^{-\gamma_0} & r < r_0 \\ \rho_0 \left(\frac{r}{r_j}\right)^{-\gamma_{j+1}} \prod_{n=1}^j \left(\frac{r_n}{r_{n-1}}\right)^{-\gamma_n} & r_j < r < r_{j+1} \end{cases}$$

DM profile can span
cusped ↔ cored

- Gaia challenge spherical mocks:
 - Plummer light profile
 - Cusped DM profile
 - Isotropic

FIDUCIAL SETUP

- Nested Plummer light profile

J.I. Read and P. Steger [1701.04833]

$$\nu(r) = \sum_{i=1}^{N_p} \frac{3M_i}{4\pi a_i^3} \times \left(1 + \frac{r^2}{a_i^2}\right)^{-5/2} \xleftrightarrow{\text{Abel transform}} \Sigma(R) = \sum_{i=1}^{N_p} \frac{M_i a_i^2}{\pi(a_i^2 + R^2)^2}$$

- Broken power law DM profile: analytic formula for enclosed DM mass

$$\rho(r) = \begin{cases} \rho_0 \left(\frac{r}{r_0}\right)^{-\gamma_0} & r < r_0 \\ \rho_0 \left(\frac{r}{r_j}\right)^{-\gamma_{j+1}} \prod_{n=1}^j \left(\frac{r_n}{r_{n-1}}\right)^{-\gamma_n} & r_j < r < r_{j+1} \end{cases}$$

DM profile can span
cusped ↔ cored

- Gaia challenge spherical mocks:

- Plummer light profile
- Cusped DM profile
- Isotropic

Analytic formulas for 2d/3d stellar density and enclosed DM mass profiles
→ more computationally tractable

FIDUCIAL SETUP

- Nested Plummer light profile

J.I. Read and P. Steger [1701.04833]

$$\nu(r) = \sum_{i=1}^{N_p} \frac{3M_i}{4\pi a_i^3} \times \left(1 + \frac{r^2}{a_i^2}\right)^{-5/2} \xleftrightarrow{\text{Abel transform}} \Sigma(R) = \sum_{i=1}^{N_p} \frac{M_i a_i^2}{\pi(a_i^2 + R^2)^2}$$

- Broken power law DM profile: analytic formula for enclosed DM mass

$$\rho(r) = \begin{cases} \rho_0 \left(\frac{r}{r_0}\right)^{-\gamma_0} & r < r_0 \\ \rho_0 \left(\frac{r}{r_j}\right)^{-\gamma_{j+1}} \prod_{n=1}^j \left(\frac{r_n}{r_{n-1}}\right)^{-\gamma_n} & r_j < r < r_{j+1} \end{cases}$$

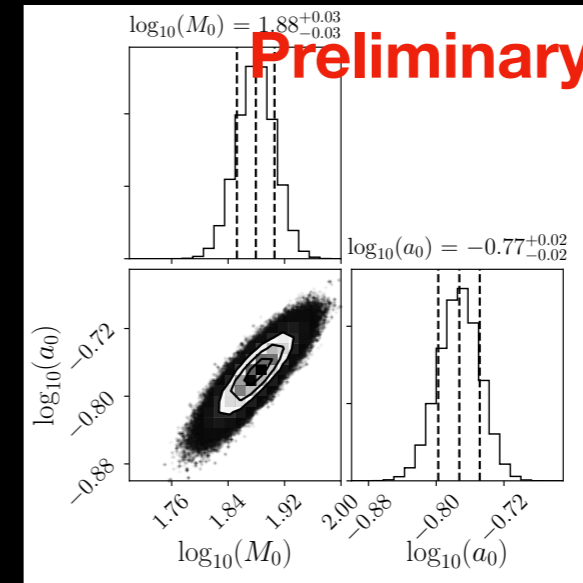
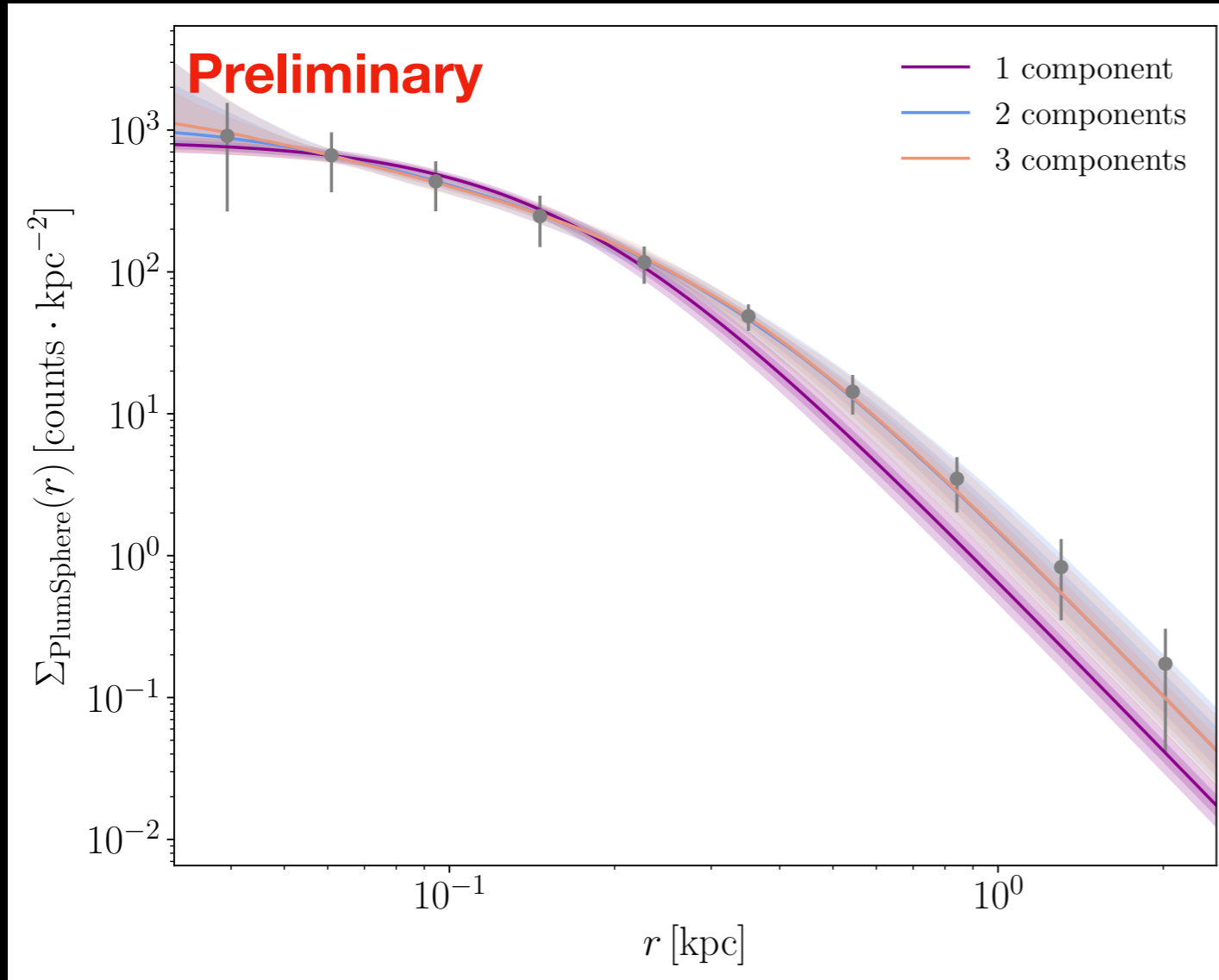
DM profile can span
cusped ↔ cored

- Gaia challenge spherical mocks:
 - Plummer light profile
 - Cusped DM profile
 - Isotropic

STEP 1: LIGHT PROFILE FIT

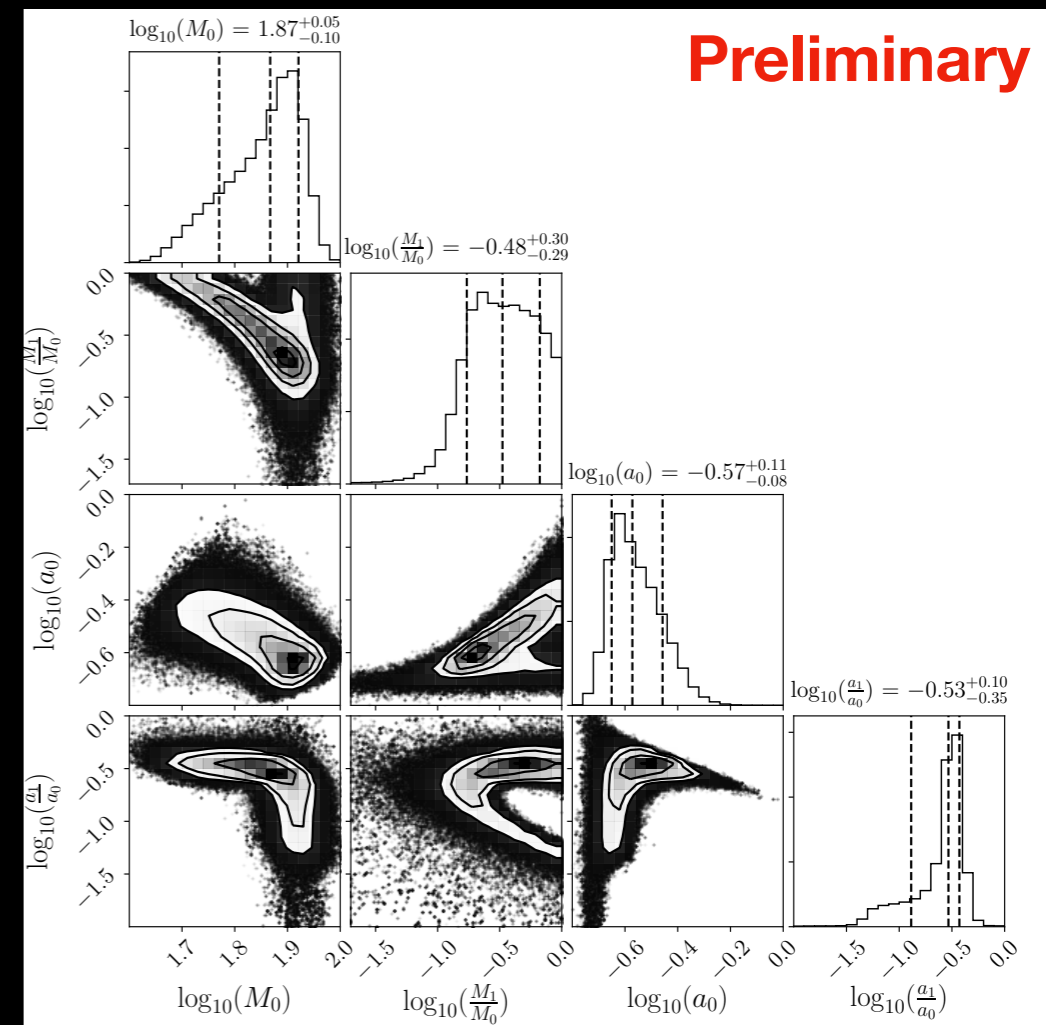
- Binned likelihood fit to stellar positions
- Fits tend to be well-constrained

100 stars



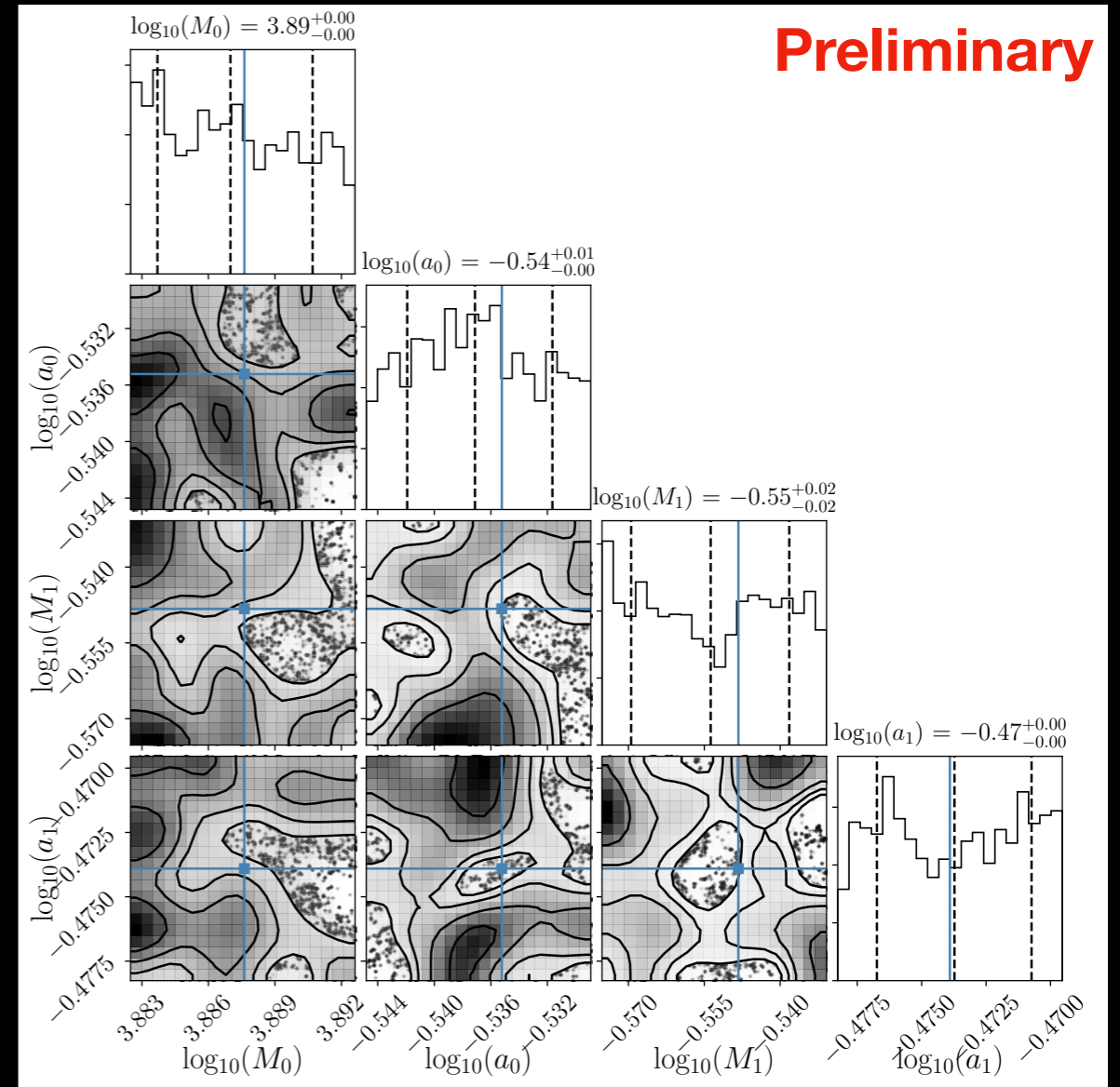
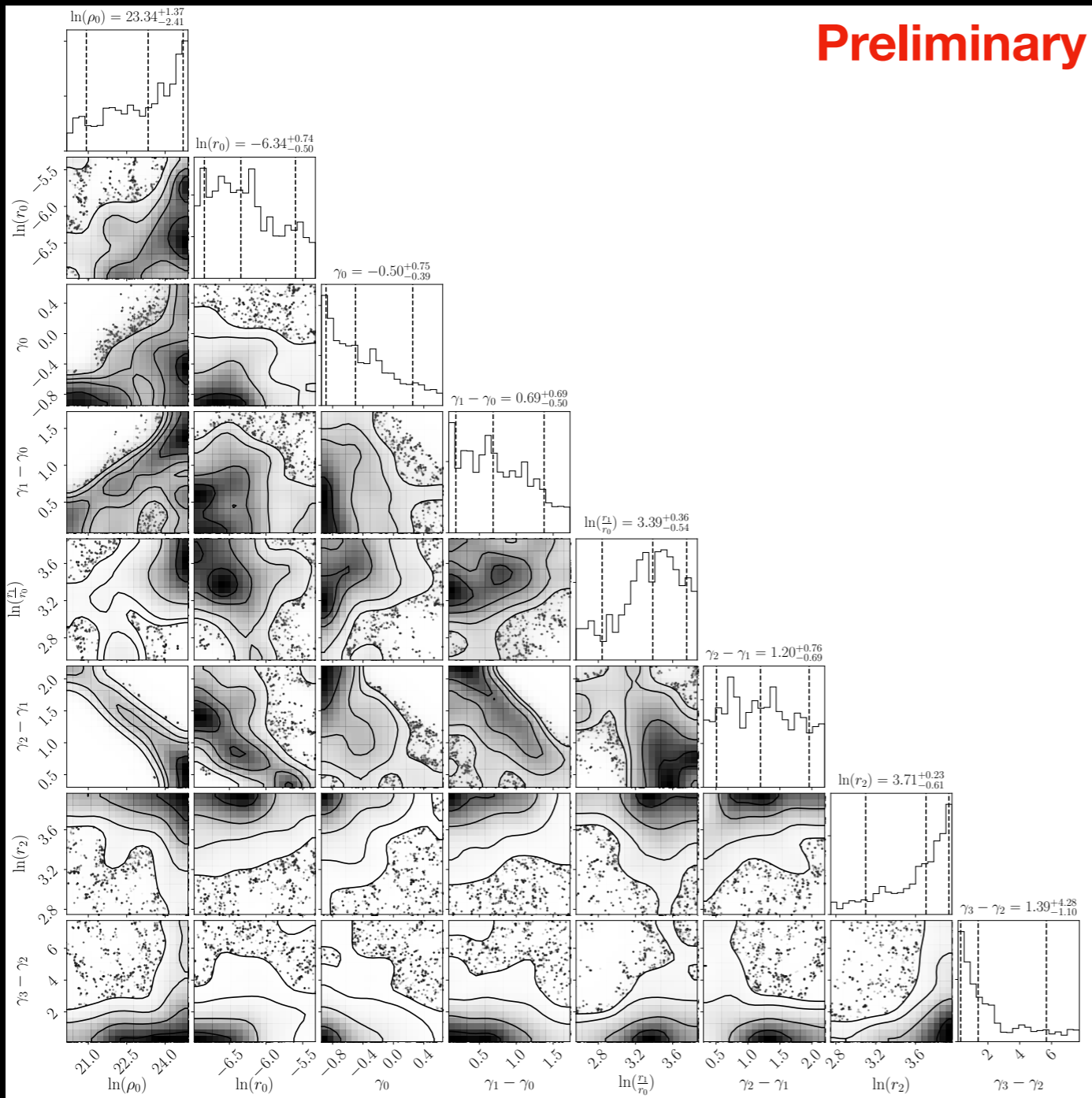
← 1 Plummer component

2 Plummer components



STEP 2: VELOCITY DISPERSION FIT

3000 stars



STEP 2: VELOCITY DISPERSION FIT

500 stars

